The Thesis Committee for Travis Zhi-Rong Wicks
Certifies that this is the approved version of the following thesis:

The Use of $\delta^{13}C$ Values of Leporid Teeth as Indicators of Past Vegetation

APPROVED BY
SUPERVISING COMMITTEE:

Supervisor:

Timothy M. Shanahan

Co-Supervisor:

Christopher J. Bell

Daniel O. Breecker

The Use of $\delta^{13}C$ Values of Leporid Teeth as Indicators of Past Vegetation

by

Travis Zhi-Rong Wicks, B.S.

Thesis

Presented to the Faculty of the Graduate School of

The University of Texas at Austin

in Partial Fulfillment

of the Requirements

for the Degree of

Master of Science in Geological Sciences

The University of Texas at Austin

May 2013

Dedication

This thesis is dedicated to my parents

who have influenced every part of who I am today.

Acknowledgements

I hate to start off with an apology, but as a disclaimer, I am sorry for the omission of anyone who deserves acknowledgement. Though I may have forgotten to include you in the acknowledgements, know that I am fully appreciative of the assistance you have provided me.

I would like to express my deepest appreciation for all the support my family has given me. My parents, Dr. Charles W. Wicks, Jr. III, and Jackie C. Wicks and my brothers, Cody Z. Wicks and Jamison Z. Wicks have provided a tremendous amount of intellectual, financial, and especially moral support. Without the support of each one of these people, whom I love dearly, I undoubtedly would have been incapable of finishing this work.

Additionally, none of this would have been conceived without the support of my committee. Though I was the one to carry out this project, Dr. Tim Shanahan and Dr. Chris Bell were the ones who conceived the project and provided tremendous guidance every step of the way. I can only hope that they feel I have done this project justice. Dr. Dan Breecker was incredibly flexible throughout this ordeal, and was always willing to sit down and talk shop when I wanted to.

The members, past and present, of the Shanahan lab were critical in the execution of every step of my project. From coring to extraction to writing to just helping me keep my sanity and sense of self-worth at reasonable levels, Veronica Anderson, Vera Stoynova, Curtis Bixler, Kyra Kim and John Swartz never seemed to not be willing to help.

Throughout all of this, Dr. Ernie Lundelius was the source of sage advice on everything from Hall's Cave to leporid teeth to cave sedimentology to who to call for bail should I end up in prison. Aside from connections, equipment, and methodological know-how, Ernie provided copious amounts of inspiration, motivation, laughter, and color (and not just blue) to my master's experience.

The help of Dr. Terry Quinn, his students, Kaustubh Thirumalai, Chris Maupin, and Meaghan Gorman, and lab tech, Dorinda Ostermann, was absolutely indispensable. The entire tooth portion of this study would have been feasible without their help.

I extend my deepest thanks to Billie Hall for allowing me onto her property to sample for bulk carbon analyses. I can safely say that Mrs. Hall was always welcoming and open to whatever we had to do. I only hope I can pay her generosity forwards someday to an aspiring scientist.

Actually obtaining samples was the work of a number of people. Without the help of Roger Gary, I would not have come up with a functional sampling protocol. Madison Ball, Chad Baber, Will Gelnaw, and Robert Burroughs were terrific field assistants, and hopefully the sore muscles, bumps, bruises, and the "goat lung" was at least partially compensated for by all the fun we had in ~~Goat Crap~~ Hall's Cave.

The actual access to the teeth was only allowed with authorization from Dr. Tim Rowe, whom I also need to thank for being the only reason I was accepted to the program in the first place. Matt Brown and Dr. Chris Sagebiel were a huge help in dealing with the collections and how I should deal with the bureaucratic aspect of destructive sampling. I have to additionally thank Allison Honea for enthusiastically going through several metric craploads of Hall's Cave matrix with me in search of elusive leporid teeth. Lastly, I need to acknowledge the tremendous work of Dr. Rick Toomey, without whom I would have no incredible Hall's Cave record to sample in the first place.

There are also a number of people I need to recognize for their instrumental, climatological, geophysical, or botanical knowhow. In no particular order I greatly appreciate this help from Dr. Toti Larson, Dorinda Ostermann, Dr. Jack Holt, Kevin Befus, Isaac Smith, Dr. Lisa Boucher, and Adam Bowerman, my go-to climatologist.

I also need to thank the folks who provided me with the many employment opportunities I took on to keep myself financially afloat during all of this. Dr. Julia Clarke, Dr. Chris Bell, and Dr. Mary Poteet are the reasons I was able to gain teaching experience here and truly discover my passion for it. Dr. Ann Molineux was my summer support, and the rest of the NPL crew, especially Angie Thompson, made great company in the shelter of the lab during blistering Austin summers.

Funding for this project was provided by the Jackson School of Geosciences, Tim Shanahan, Chris Bell, and the Lundelius Scholarship. I certainly would not have been able to pay for this on my own, and am incredibly thankful that others were so giving.

I would like to thank my fellow UT paleontology students and associates for more reasons than I can possibly list here. In no particular order, this includes Rachel Simon, Robert Burroughs, Will Gelnaw, Alicia Kennedy, Michelle Stocker, James Profitt, Lauren English, Ashley Latimer, Natasha Vitek, Josh Lively, Zhiheng Li, Adam Marsh, Zachary Morris, Felicia Kulp, Katie Brown, Gerard Wallace, Dr. Sterling Nesbitt, Dr. Matthew Colbert, Katherine Criswell, Dr. Jennifer Olori, Christian George, Drew Eddy, and Kyle Womack.

Lastly, I would like to thank Aubri Kottek, who supported me in all the intangible ways a human could. She was my main source of happiness during these years, and is the one who could pull me out of the pit of self-loathing and depression I would occasionally slip into.

Abstract

The Use of $\delta^{13}C$ Values of Leporid Teeth as Indicators of Past Vegetation

Travis Zhi-Rong Wicks, M.S.

The University of Texas at Austin, 2013

Supervisor: Timothy M. Shanahan

Co-Supervisor: Christopher J. Bell

Records of change of $\delta^{13}C$ values in vertebrate teeth offer an opportunity to gain insight into changes in past vegetation. Increasingly, teeth from small mammals are used for such purposes, but because their teeth grow very rapidly, seasonal changes in vegetation potentially provide a large source of variability in carbon isotope composition, complicating interpretations of small mammal tooth isotope data. To investigate the controls of seasonality on the stable isotope composition of fossil teeth, we constructed a Monte-Carlo-based model to simulate the effects of changes in the seasonal pattern of diet in leporid lagomorphs (rabbits and hares) on the distribution of $\delta^{13}C$ values in random populations of leporid teeth from the Edwards Plateau in central Texas. Changes in mean-state, seasonal vegetation range, and relative season length manifest themselves in predictable ways in the median, standard deviation, and skewness of simulated tooth $\delta^{13}C$ populations, provided sufficient numbers of teeth are analyzed. This Monte Carlo model was applied to the interpretation of a 20,000 year record of leporid tooth $\delta^{13}C$ values from Hall's Cave on the Edwards Plateau in central Texas. Variations in the $\delta^{13}C$

values of teeth deposited at the same time (standard deviation = 1.69‰) are larger than changes in the mean vegetation composition reconstructed from bulk organic carbon $\delta^{13}C$, indicating the influence of short-term variability, making it difficult to assess changes in mean C_3/C_4 vegetation from the tooth $\delta^{13}C$ data. However, populations of teeth from different climate intervals (e.g., the late Glacial, Younger Dryas, and the Holocene) display changes in the shape of the tooth $\delta^{13}C$ distributions. Interpretation of these changes as shifts in seasonal vegetation patterns that are based upon results from our model are consistent with hypothesized climatic changes. An increase in the standard deviation of the tooth population between the late Glacial and the Younger Dryas – Holocene is consistent with an increase in seasonality. Furthermore, a shift to more C_3-dominated vegetation in the tooth $\delta^{13}C$ distribution during the Younger Dryas is accompanied by a more skewed population – indicative of not only wetter conditions but an increase in the duration in the C_3 growing season. However, late Holocene changes in vegetation are not clear in the tooth data, despite the evidence from bulk organic carbon $\delta^{13}C$ values for an increase in % C_3 vegetation of 57%. Small mammal teeth can potentially provide unique insights into climate and vegetation on seasonal and longer timescales that complement other data, but should be interpreted with a careful consideration of local conditions, taxon ecology and physiology, and the dominant timescales of isotope variability.

Table of Contents

List of Tables xii

List of Figures xiii

1 Introduction 1

2 Study Area 5

2.1 Hall's Cave 5

2.2 Modern Climatology and Vegetation 6

3 Methods 8

3.1 Modeling the effect of intra-annual variability on leporid tooth isotopic composition 8

3.1.1 Establishing the Seasonal Cycle in Leporid Tooth $\delta^{13}C$ Values 9

3.1.2 Modeling variations in vegetation seasonality 12

3.2 Sediment Sampling 14

3.3 Chronology 15

3.4 Isotope Analyses 16

3.4.1 Bulk Organic Carbon 16

3.4.2 Leporid Enamel Carbon 17

4 Results and Discussion 19

4.1 Model Results 19

4.1.1 Mean-State Shift 19

4.1.2 Change in Seasonal Range 20

4.1.3 Change in Relative Season Length 21

4.1.4 Inferring Changes in the Seasonal Cycle from Distribution Changes 22

4.1.5 Error and Testing for Significance 24

4.2 Variability on Longer Time Scales 27

4.3 Variations in Leporid Teeth $\delta^{13}C$ Values from Hall's Cave 29

4.3.1 Tooth $\delta^{13}C$ Variability 31

4.3.2 Offset in C_3/C_4 Vegetation....33
4.3.3 Changes in leporid $\delta^{13}C$ distributions....34
4.3.4.1 Late Glacial Variability....34
4.3.4.2 Younger Dryas Variability and Median....35
4.3.4.3 Lack of Holocene Change....37
5 Implications for Interpreting $\delta^{13}C$ values of Small Mammal Teeth....40
6 Figures and Tables....43
7 Appendices....54
Appendix A: Supplemental Tables....54
Appendix B: Matlab Modeling Scripts....73
Script 1: Distribution change with relative season length....73
Script 2: Distribution change with amplitude....77
Script 3: Precision change with sample size....81
References....86

List of Tables

Table 1: Probabilities of detection 53

Table S1: Leporid tooth $\delta^{13}C$ values 54

Table S2: Bulk organic carbon isotope data.....60

Table S3: Radiocarbon dates as published by Cooke et al. (2003). 67

Table S4: Age-depth model. 68

List of Figures

Figure 1: Modern climate and vegetation of Texas.....43

Figure 2: Modern seasonal climate and vegetation of the study area.....44

Figure 3: Anatomy of and possible changes to intra-annual changes in vegetation.....45

Figure 4: Age model of Hall's Cave deposit.....46

Figure 5: Contour plots representing changes in median.....47

Figure 6: Sample size requirements.....48

Figure 7: Application of errors.....50

Figure 8: Summary of enamel carbon isotope measurements.....52

1 Introduction

Reconstructions of past vegetation are important for understanding past ecosystem dynamics and climate variability. Carbon isotope variations in vertebrate teeth are widely used as tools for reconstructing past vegetation (e.g., Lee-Thorp and Beaumont, 1995; MacFadden et al., 1996; Cerling et al., 1997; Koch et al., 2004; Forbes et al., 2010; Bedaso et al., 2013), particularly in regions such as central Texas, where there are few well-resolved and long-term records of past vegetation change. Because the stable carbon isotopic compositions of herbivore teeth are determined largely by the diet of the animal, offset by a predictable magnitude as a result of physiological processes (DeNiro and Epstein, 1978; Cerling and Harris, 1999), the $\delta^{13}C$ values of herbivore teeth can be used to reconstruct changes in the relative abundance on the landscape of C_3 and C_4 photosynthetic plants, assuming no dietary preference.

To date, most stable isotope studies of herbivore teeth have focused on the teeth of large, herbivorous mammals because the enamel is both easy to sample and its isotopic composition integrates diet over at least a year (Cerling and Sharp, 1996; Hoppe et al., 2004; Feranec et al., 2009). Though they are less well studied, small mammals are increasingly being used to tackle questions about paleoenvironmental change (e.g., Rogers and Wang, 2002; Feranec et al., 2010; McLean and Emslie, 2012; Hynek et al., 2012). The use of small mammals confers several advantages over large mammals, such as the greater relative abundance of small mammals in the fossil record (e.g., Hibbard 1949). Small mammals also are typically non-migratory, ensuring that $\delta^{13}C$ values do not

reflect a mixed signal associated with changes in the isotopic composition of vegetation across regional climate gradients. For example, leporid lagomorphs (rabbits and hares) typically spend their lives in areas 0.4-200 ha in size (McNab 1963; Chapman and Willner 1978), but large mammals such as *Bison* have modern home ranges several orders of magnitude larger (Larter and Gates, 1994), and are known to migrate long distances (Morgan, 1980; Feranec et al., 2009). Leporids also often are generalist herbivores (Feldhamer et al., 2003), so their teeth reflect a more representative proportion of the extant vegetation, namely low lying herbaceous plants, than large, grazing herbivores, such as *Bison* and *Equus*, which primarily consume grasses (Feldhamer et al., 2003). Another common feature of small, herbivorous mammals is hypselodont (ever-growing) dentition (Ungar 2010). When sampled from adults, these teeth are less likely to reflect the nursing period, which can result in a carbon isotope value that is (0-5.1‰) lighter than expected from the adult diet (Hobson and Sease 1998; Jenkins et al., 2001).

However, hypselodont small mammal teeth are fast-growing (0.6-1.6 mm/day) (Podlesak et al., 2008), resulting in tooth isotopic compositions that are drawn from half to one month of the animal's diet. Any isotopic measurements of these teeth will therefore represent snapshots of vegetation consumed by the animal 2-4 weeks prior to death. This can result in variations in tooth $\delta^{13}C$ values depending on the time of the year the tooth stopped growing. Because seasonal changes in C_3/C_4 composition in arid regions can be large (e.g., a seasonal range of 25% to 100% C_3 vegetation on the Edwards Plateau, see Fig. 2c), these variations are as large as the changes in landscape C_3/C_4 biomass being reconstructed. As a result, it may be difficult, if not impossible, to

gain useful information on past vegetation changes using long-term variations in the $\delta^{13}C$ values of individual small mammal teeth.

An alternative approach is to study changes in the distributions of $\delta^{13}C$ values from populations of small mammal teeth over time. Provided sufficient number of teeth are sampled to characterize the statistics of the tooth populations, changes in these statistics should reflect not only changes in the mean vegetation growing on the landscape, but also changes in the seasonality of vegetation. Such an approach was recently suggested for interpreting the $\delta^{18}O$ values of rodent dentition (Royer et al., 2013).

A similar approach has been used with to reconstruct sea surface temperature variability using the $\delta^{18}O$ values of single foraminifera (SST; Koutavas et al., 2006; Leduc et al., 2009; Koutavas and Joanides, 2012). In the single-foram approach, populations of single foraminifera $\delta^{18}O$ values from discrete intervals of sedimentation are generated, and changes in the standard deviations of these distributions are interpreted as reflecting changes in the magnitude of SST variability associated with the El Nino Southern Oscillation (ENSO). Recently, several models were created to investigate how sample size and long-term climate trends affect the resulting distribution of measured isotopic values, as well as to aid in the interpretation of paleoclimate reconstructions based on single-foram analyses (Leduc et al., 2009; Thirumalai et al., pers. comm.). These exercises have demonstrated the need for modeling approaches in order to properly understand and interpret the controls on changes in single-foram populations.

In the present study, we investigate the utility of using a similar approach to understand and interpret the $\delta^{13}C$ values of populations of individual, fast-growing, fossil leporid teeth as indicators of past seasonal variability in vegetation. Methods similar to those developed for single-foraminifera are used to simulate how changes in the C_3/C_4 seasonal cycle affect populations of leporid $\delta^{13}C$ values, and synthetic leporid $\delta^{13}C$ populations are sub-sampled to examine the relationship between sample size and ability to approximate characteristics of the total population. Changes in the seasonal characteristics of the vegetation available to leporids are modeled, and the results are used to understand how changes in seasonality manifest themselves in changes in the in the distributions of leporid tooth $\delta^{13}C$ values. Those results are then applied to the contruction of vegetation changes from leporid tooth $\delta^{13}C$ data from the sediments of Hall's Cave, a continuous record of past sedimentation on the Edwards Plateau spanning the last 20,000 years.

2 Study Area

2.1 HALL'S CAVE

Hall's Cave is located in central Texas near the center of the Edwards Plateau, a large, karstified, limestone plateau (30°8'0.53"N 99°32'15.30"W) at 695 m elevation above sea level (Fig. 1c). The cave currently consists of a single chamber approximately 30 m x 55 m in the Segovia Member of the Lower Cretaceous Edwards Limestone (Toomey 1993). The floor is covered by up to 3.7 m of well-stratified, fossiliferous sediment (Toomey 1993). Excavations in the northern portion of the cave approximately 10 m from the entrance were carried out in multiple pits, now collectively called Composite Pit I. The majority of that pit was excavated by Rick Toomey at 5 cm intervals from 1986-1993, and the fossils removed from the site currently reside at the Vertebrate Paleontology Laboratory at the University of Texas at Austin (Toomey 1993).

The current entrance to the cave is a talus slope located in the northeastern corner, and sediments are washed into the cave during precipitation events. Sediments are primarily fine-grained clays, soils, and sands, with limestone and chert cobbles present as well as occasional boulders. Considerable biological contributions to the deposit also are present in the form of guano, feathers, charcoal, plant macrofossils, and bone. The majority of vertebrate skeletal material was deposited via owl pellet accumulation, though occasional large mammal remains were likely deposited through a different mechanism (Toomey 1993). Currently, we know of no modern owl species on the Edwards Plateau that is both migratory and large enough to eat an adult leporid

(Johnsgard, 2002), leading us to hypothesize that any seasonal component to adult leporid deposition was minimal.

2.2 Modern Climatology and Vegetation

The climate of the region surrounding Hall's Cave is subtropical and subhumid (Larkin and Bomar, 1983) with a mean annual temperature of 18.4^{o}C, and monthly mean temperatures range from 8.3^{o}C (January) to 27.4^{o}C (August) (Fig. 2a), based on 30-year climate normals from Kerrville from the National Climate Data Center (Arguez et al., 2012). Mean annual precipitation is 814 mm and monthly precipitation totals range between 40 mm in January and 102 mm in May (Durre et al., 2012). The majority of that moisture comes from the Gulf of Mexico, with input from occasional storms from the east Pacific (Bomar 1995). The area experiences two maxima in precipitation during the late spring/early summer and the early fall, with little precipitation occurring in the winter and summer (Fig. 2b). Much of the precipitation that falls during the late spring and summer comes in the form of nocturnal thunderstorms that are driven by a low-level southerly flow from the Gulf of Mexico called the Great Plains low-level jet (Means, 1952; Mitchell et al., 1995).

The vegetation surrounding Hall's Cave is characterized as oak savanna and is largely composed of C_4 summer grasses and evergreen C_3 shrubs and trees (Fowler and Dunlap, 1986). C_3 forbs grow in significant abundance during spring months, and one species of C_3 grass, *Nassella leucotricha*, grows during the fall, winter, and spring months. CAM phosotynthesizers, such as *Opuntia* and other succulents, appear on the

landscape year-round in small numbers. These seasonal patterns of growth result in large changes in C_3/C_4 biomass through the year with C_4 biomass dominating the late spring through fall (Fig. 2c). C_3 vegetation is highest in relative abundance during the winter and early spring, and maintains a noticeable presence throughout the rest of the year as woody plants and a few species of perennial forb species (Correll and Johnston, 1970; Fowler and Dunlap, 1986). Because of these seasonal changes in C_3/C_4 abundance, changes in seasonal climate patterns have the potential to affect the overall proportion of C_3/C_4 plants. This is evident in the correlation between C_4 abundance and the proportion of precipitation occurring during the summer, the primary C_4 growing season (Paruelo and Lauenroth 1996).

Gradients in vegetation and climate across the Edwards Plateau are characteristic of those exhibited across the state of Texas. The modern climatology is largely defined by a strong east-to-west precipitation gradient and a latitudinal temperature gradient (Fig. 3a,b). Spatial differences in mean annual precipitation (MAP) exert a strong effect on the composition of vegetation with higher amounts of tree cover occurring in portions of the state with greater MAP (Fig. 3c). This is expected because MAP has been shown to correlate with tree cover in subtropical and tropical grasslands and savannas (Sankaran, 2005; Bond, 2008). Because trees are C_3 photosynthesizers (Sage et al., 2011), and the vast majority of grasses on the Edwards Plateau are C_4 plants (Smeins et al., 1976; Fowler and Dunlap 1986), changes in the proportion of tree cover on the landscape will manifest itself as changes in the proportion of C_3/C_4 plants and the biomass-weighted mean $\delta^{13}C$ value of the vegetation.

3 Methods

3.1 Modeling the effect of intra-annual variability on leporid tooth isotopic composition

Because many small mammals, like leporids, growth their teeth very rapidly, the stable isotope signal in these teeth reflects at most a few weeks to a month of time. As a result, the isotopic signal in small mammal teeth is strongly affected by seasonal variations in vegetation availability. In places like the Edwards Plateau, where seasonal vegetation changes are large, this effect imparts significant variation on the signal contained in individual teeth. However, if populations of individual teeth can be analyzed from discrete time intervals, the distribution of tooth $\delta^{13}C$ values within this population can potentially provide additional information about the variations in vegetation composition within that sampling interval. Furthermore, if the total range in the seasonal cycle of vegetation is large, the seasonal cycle could potentially dominate the isotope signal and tooth population data will provide insights into changes in seasonality.

To better understand these processes, and to provide a framework for interpreting leporid tooth population data, we developed a Monte-Carlo model for simulating the production of teeth from a synthetic population of leporids living on the Edwards Plateau with the modern seasonal cycle of vegetation. By sampling the synthetic "true" population of teeth produced under these conditions, and by altering the seasonal vegetation cycle, this approach offers a means of investigating how changes in vegetation manifest themselves in tooth $\delta^{13}C$ distributions and allows us to set guidelines for

estimating the number of teeth needed to characterize the population and the influence of sample size on the robustness of our data interpretations.

3.1.1 Establishing the Seasonal Cycle in Leporid Tooth $\delta^{13}C$ Values

To model the incorporation of seasonal vegetation changes into leporid tooth $\delta^{13}C$ values, it is necessary to understand the seasonal cycle in C_3/C_4 vegetation, how that vegetation is sampled by leporids, and how that signal is incorporated into tooth $\delta^{13}C$ values. First, existing data on the relative abundances of different species of plants on the Edwards Plateau were gathered (Fowler and Dunlap, 1986), and each species of plant was designated as utilizing the C_3 or C_4 photosynthetic pathway (Van Auken, 1997; Christin et al., 2008; Besnard et al., 2009; Sage, 2011). Growing season ranges for each plant species (Correll and Johnston, 1970) were then applied, allowing us to construct a synthetic monthly record of C_3/C_4 vegetation changes on the Edwards Plateau (Fig. 2c). The data exhibit a period of C_3 dominance in the winter and C_4 dominance in the summer and fall, with transitional periods occurring in the early winter/late fall and spring. This general cycle of increased C_4 growth during warmer portions of the year and C_3 dominance during cooler portions is consistent with observations reported elsewhere (Ode and Tieszen, 1980; Tieszen et al., 1980).

Estimated C_3/C_4 vegetation percentages were converted into mean landscape $\delta^{13}C$ values assuming mean values for C_3 (-27‰) and C_4 (-13‰) plants (Boutton et al., 1998). Though plants with the same photosynthetic pathway will have different isotopic composition due to species differences (Cerling and Harris, 1999), the $\delta^{13}C$ value of CO_2

(Keeling et al., 2005), changes in irradiance (Ehleringer et al., 1986; Zimmerman and Ehleringer, 1990), water stress (Ehleringer, 1993), and even the structure of the surrounding vegetation (Medina et al., 1986), they provide reasonable estimates which, when applied to our estimates of C_3/C_4 percentages from modern vegetation data, allow us to create a general estimate of the seasonal cycle in plant $\delta^{13}C$ on the Edwards Plateau. Furthermore, for the purposes of this model, the numerical $\delta^{13}C$ value of consumed vegetation is less important than how changes in the proportion of C_3/C_4 vegetation are manifested in $\delta^{13}C$ values and as a result in the distribution of teeth produced by leporids consuming this vegetation.

Modelling of the incorporation of this idealized seasonal vegetation signal into leporid teeth necessitates a consideration of the possible sources of differences in carbon isotope composition between leporid teeth and vegetation on the landscape. These include seasonal changes in diet, dietary preferences, carbon isotope fractionation during metabolism and tooth production, and individual, random variability due to a combination of plant selection and microenvironments. Leporids are expected to consume vegetation which reflects the seasonal pattern in C_3/C_4 plant abundance that is present on the landscape. As leporids are not obligate drinkers, they largely consume vegetation according to moisture content (Dalke and Sime, 1941; Turkowski, 1975; Brewer, 2006; Ugan and Coltrain, 2011). Plants contain highest moisture content when growing, so we expect leporid diet during a given time to be largely dependent on what is actively growing on the landscape. Because they also do not store food or hibernate, leporids sample the vegetation year-round (Vander Wall, 1971; Feldhamer et al., 2003).

However, the absolute proportion of C_3/C_4 consumed is not expected to match precisely that in the environment because leporids have a tendency to favor certain plant types over others. For example, woody plant material is rarely consumed unless other vegetation types are scarce (Schmidly, 1994). Additionally, during the spring on the Edwards Plateau, when both C_3 forbs and sedges and C_4 grasses are growing (Correll and Johnston, 1970; Fowler and Dunlap, 1986), isotopic analyses reveal that C_3 forbs are preferentially consumed (Smith, 2011). Because of this, the proportion of C_3/C_4 consumed is likely somewhat offset from the true composition of vegetation on the landscape. Though the direction of the offset will remain the same as vegetation composition changes, the amount of offset will likely change, potentially complicating the interpretations of leporid tooth distributions. Although the magnitude of this effect is unknown, the dietary preference amongst modern leporids is relatively small, so for the purposes of this modeling exercise, we assume that it is small. This is consistent with the limited data from modern leporids, which show variations of ±1.59‰ in $\delta^{13}C$ for animals living at the same time and in the same location (Smith, 2011). This was incorporated into the model as a randomizing element in the generation of simulated tooth $\delta^{13}C$ values.

Additional offsets between the $\delta^{13}C$ values of the vegetation on the landscape and tooth $\delta^{13}C$ also reflect the isotope fractionation between the food source and the tooth material. Previous studies on leporids have reported offsets of ca. + 12.8‰ (Passey et al., 2005).

3.1.2 Modeling variations in vegetation seasonality

In order to understand better how seasonal changes in vegetation would influence the $\delta^{13}C$ signal incorporated into leporid teeth, we considered three main avenues by which the vegetation might change on a seasonal basis: (1) a change in the mean-state, (2) a change in the seasonal range, and (3) a change in season length. For simplicity, we first consider these changes individually, and then discuss the influence of combined effects later.

The first of these, a change in the mean-state, is modeled as a shift towards a greater or lower proportion of C_3 vegetation, with no direct change in the seasonal cycle. This type of change would be analogous to a situation in which an overall increase or decrease in mean annual temperature or precipitation resulted in an increase or decrease in the proportion of woody plants in the landscape without any change in the seasonal distribution of plants (Fig. 3b). For example, an increase in precipitation during all months might be anticipated to generate a corresponding increase in the relative proportion of C_3 plants during all months.

The second possible vegetation change that was considered is a change in the seasonal proportion of C_3/C_4 plants (Fig 3c). This type of change might include a change in the composition of plants in the winter with no change in the summer, a change in summer vegetation without any change in winter, differential change in both seasons in the same direction, or a change in both seasons in the opposite direction. End-member conditions for this change would be 100% C_4 in summer and 100% C_3 in winter, or, conversely, a constant vegetation composition thoughout the year. In some cases, these

changes could result in a shift in the annual average C_3/C_4 ratio; in other cases, they would not be associated with a change in the mean-state. Because a change in the mean-state is modeled as a separate condition, only seasonal range changes that do not result in a mean-state shift were considered. These changes in the seasonal range of vegetation composition would be consistent with an increase or decrease in climate seasonality. Because the timing of deciduous/annual plant dormancy/death depends on environmental cues, such as aridity, photoperiod, and temperature (Volaire and Norton, 2006; Rohde and Bhalerao, 2007), changes in the magnitude of climatic seasonality could result in changes in the amount of C_3 and C_4 plants that grow through the C_4 and C_3 seasons, respectively. This is evident in the correlation between minimum temperature during the growing season and $\%C_4$ grasses observed in North America today (Teeri and Stowe 1976).

The third possible vegetation change was a shift in the relative lengths of the C_3 and C_4 growing seasons (Fig. 3d). This could include a change in the timing of dormancy termination/germination or dormancy/death of C_3 or C_4 plants, resulting in the growth of C_3/C_4 vegetation during a longer or shorter part of the year. Because relative season lengths that approach 100% C_4 or 100% C_3 growth are unrealistic in our study area, we restricted the possible end-member season lengths to between 20% and 80%. Such changes could result from changes in the time of year that certain environmental thresholds are crossed. For example, because temperatures play a large role in timing of germination (Angevine and Chabot, 1979; Probert, 2000), lower overall temperatures

could truncate the amount of the year that C_4 plants are capable of growing, shortening the C_4 season relative to the C_3 season.

3.2 SEDIMENT SAMPLING

A continuous record of the upper 2 m of sediment in Hall's Cave was obtained by coring approximately 10 cm from the northwest edge of Pit 1d/e (Toomey, 1993) in January, 2012. The bottom meter (2-3 m depth) was not obtained from this portion of the cave due to large limestone clasts inhibiting sediment collection. Instead, the remainder (~1 m) was obtained by coring approximately 10 cm from the northeast edge of the same pit during a subsequent trip in July, 2012. Overlap between the two sections was identified using changes in lithostratigraphy and reference nails left in the wall of the pit during the first visit. An unconformity in the sediment was identified at 222-236 cm by the presence of hair and goat feces indicative of modern sediment. This was likely due to sloughing off of the side of Toomey's original excavation and subsequent backfilling, and the interval was excluded from the analyses. A sudden change in the character of the sediment from red clay to dark brown and black organic materials along with the presence of numerous articulated bat fossils below 287 cm depth were indicative of a guano deposit. This interval was also excluded from analyses.

Because the cave sediment samples were obtained separately from the fossil tooth samples and associated radiocarbon dates, it was necessary to correlate sample depths between the sediment cores and the depths of the tooth samples as documented by

Toomey (1993) in order to put them on the same age-depth chronology. To do so, we used a series of reference nails placed in the wall of the pit by Stafford (Cooke et al., 2003) at 0, 1.0, and 1.5 m depth. These depth correlations were confirmed by measuring a plumb line from a level-line extended from a railroad spike datum driven into the wall closest to the pit, also placed by Toomey in 1993. Lithostratigraphic boundaries were used to provide additional ties to Toomey's section.

3.3 CHRONOLOGY

The chronologic control of this deposit is based on 23 radiocarbon dates of charcoal, humates, and bone collagen (Fig. 4; Table S3; Cooke et al., 2003). Age modeling was performed using the Bayesian age-depth modeling program BACON (Table S4; Blaauw and Christen, 2011). ^{14}C dates were converted to calendar ages using the IntCal09 calibration curve (Reimer et al., 2009). BACON uses an assumed probability distribution of sediment accumulation rates and generates a distribution of possible age-depth models considering this accumulation rate probability function and using the non-normal probability distributions for the calibrated radiocarbon ages. The output provides an estimate of both the optimal age depth model and the uncertainty in age model as a function of depth. For the Hall's Cave model, 71, 5-cm-thick sections and a mean accumulation rate of 52 year/cm were utilized. Average uncertainty was ±511 Cal. yr BP and ranges from ±165 to ±960 Cal. yr BP. Despite the wide range in uncertainty, there is no discernible trend with age, and it generally fluctuates between ±200 and ±700 Cal. yr BP throughout the section.

3.4 ISOTOPE ANALYSES

3.4.1 Bulk Organic Carbon

The stable isotopic composition of the bulk organic carbon from Hall's Cave was analyzed continuously at centimeter resolution (equivalent to 59 ±49 years) over the top 3 m. The sediment samples were homogenized with a mortar and pestle and dried either through lyophilization or in an oven at 70^{o}C for 48 hours. 2-20 mg of each sample were then placed in silver capsules, and 2-3 drops of sulfurous acid (6.4%) were applied to each vessel to remove inorganic carbon (Steinbeiss et al., 2008). Samples were again dried at 70^{o}C for 48 hours and subsequently combusted in an elemental analyzer (Costech Instruments Elemental Combustion System 4010) connected to an isotope ratio mass spectrometer (Thermo Scientific Delta V Plus). The analytical precision for these data is ±0.24‰ based upon repeated measurements of an in-house standard, which was used to correct raw measured values to the VPDB scale. The bulk sediment organic carbon $\delta^{13}C$ record is interpreted as reflecting the $\delta^{13}C$ value of the surrounding vegetation at the time of deposition with little to no isotopic enrichment during diagenesis (Balesdent et al., 1993), and provides a record of changes in the relative abundance of C_3/C_4 plants to which we can compare our tooth isotope data.

3.4.2 Leporid Enamel Carbon

Adult leporid cheek teeth were selected from among fossils excavated by Toomey (1993) and currently curated as part of the Texas Natural Science Center at the University of Texas at Austin. Upper cheek teeth were preferentially selected because of the ease of identification to Leporidae and because the thick, smooth enamel band along the mesial surface maximizes the ease of sampling. Because isolated cheek teeth are not identifiable beyond Leporidae, it is likely that multiple species were sampled. However, this problem is somewhat alleviated by the similarity of diet among the different species of leporids present across Texas today (Schmidly, 1994; Feldhamer et al., 2003). Furthermore, teeth were selected to be similar in size (~1 cm in length) to minimize the amount of taxonomic mixing among sampled teeth.

Even at the high density of fossils in the deposit, there were not enough teeth at each level to treat each excavation level (~5 cm) as a distribution. Instead, the bulk organic carbon record was used to identify four key vegetation regimes, and the 136 leporid teeth measured during this study were binned within these intervals (Fig. 7). These intervals were identified as the late Holocene (LH; n = 38), early Holocene (EH; n = 35), Younger Dryas (YD; n = 34), and late Glacial (LG; n = 29). 136 teeth were selected from levels interspersed throughout these intervals. Prior to sampling, occlusal, mesial, and lingual surfaces were photographed for archival purposes. A fine file was then used to remove contaminants and cementum that may have been on the mesial surface of each tooth. Teeth were mounted to acrylic glass using epoxy and placed on computer-controlled stage which allowed for precise control of drilling location and

depth. Approximately 0.2 mm of the mesial enamel band was removed using a carbide dental drill bit (head diameter: 0.25 mm) in a rotary tool.

Pretreatment methods were derived from those detailed by Koch et al. (1997). To remove all organic contaminants, powdered samples were treated with 2% NaOCl for 24 hrs at 0.4 mL solution/mg sample. The NaOCl solution was then decanted, and the powders were rinsed 5 times with 18MΩ water. Samples were then soaked in 0.1M acetic acid for 24 hrs at 0.4 mL solution/mg sample to remove adsorbed diagenetic carbonate. The acetic acid was decanted and the powders were rinsed 5 times with 18MΩ water. Samples were lyophilized and then reacted with phosphoric acid in an evacuated vessel in an automated carbonate preparation system (Thermo Scientific Kiel IV Carbonate Device) attached to an isotope ratio mass spectrometer (Thermo Scientific MAT 253). The analytical precision for these data is ±0.025‰ based upon repeated measurements of an in-house standard, which was used to correct raw measured values to the VPDB scale.

4 Results and Discussion

4.1 Model Results

To establish an interpretive framework for linking changes in the seasonal cycle of consumed C_3/C_4 vegetation to changes in leporid tooth $\delta^{13}C$ distributions, our synthetic populations of tooth $\delta^{13}C$ values were created using estimated seasonal vegetation patterns and dietary preferences. The distribution of $\delta^{13}C$ values for each population was characterized using median, standard deviation, and skewness. These three descriptive statistics were tracked as the seasonal dietary pattern was modified through mean-state shifts, changes in seasonal range, and changes in relative season length. The median was used to describe the distribution instead of the mean because it is the more appropriate statistic for describing the skewed distributions (Whitlock and Schluter, 2009).

4.1.1 Mean-State Shift

Because shifts in the mean-state move the entire seasonal dietary cycle towards a larger or smaller proportion of C_3 to C_4 vegetation, these dietary changes are manifested as shifts in tooth $\delta^{13}C$ distributions towards higher or lower median $\delta^{13}C$ values. In most cases, the shift in median $\delta^{13}C$ values will be the same size as that of the mean-state shift.

The potential effect of changes in the mean-state on skewness and standard deviation depend on the seasonal range in C_3/C_4 vegetation. If the seasonal range is small enough that neither season is saturated with an end-member, skewness and standard

deviation generally remain unaffected because most mean-state shifts do not change the shape of the tooth $\delta^{13}C$ distribution. In contrast, when seasonal range causes a portion of the year to abut against the end-member C_3 or C_4 vegetation values (e.g., 100% C_3 or C_4), a portion of the seasonal cycle might not be able to shift because it is already saturated with C_3 or C_4 vegetation. Because of the limited C_4 growing season and consequent C_3 dominance of C_3 vegetation during the winter, this is the most likely situation for a mean-state shift. This can cause parts of the year to accumulate on one end-member, changing the shape of the seasonal vegetation cycle and tooth $\delta^{13}C$ distribution. As the distribution shifts towards 100% C_3 or C_4 during part of the year, the distribution becomes more asymmetric. The absolute value of skewness increases until a large percentage of the year is saturated with 100% end-member values, beyond which the absolute value of skewness decreases towards zero. This results in a greater proportion of the year being on the same side of the midpoint as the saturated portion of the year. At the same time, the standard deviation decreases because the overall range of $\delta^{13}C$ values decreases. This is effectively a mean-state shift driving a simultaneous change in seasonal range and relative season length, the effects of which are discussed below. Median values continue to shift with the mean-state, but no longer track it on a permil basis.

4.1.2 Change in Seasonal Range

Shifts in the range of $\delta^{13}C$ values of vegetation over the seasonal cycle modulate the spread in tooth $\delta^{13}C$ values. The primary effect of this is to cause a change in the standard deviation of leporid $\delta^{13}C$ values (Fig. 5b). At the minimum possible seasonal range (0‰), the $\delta^{13}C$ of consumed vegetation does not change seasonally, and the spread

in leporid $\delta^{13}C$ values entirely the result of random variation in tooth values (i.e., 1.59‰). In contrast, a maximum difference in vegetation $\delta^{13}C$ changes over the course of a year (14‰), in which vegetation is 100% C_3 in winter and 100% C_4 in summer can result in a maximum standard deviation of 5.20‰. At equal relative season lengths, changes in seasonal range have no effect on median or skewness (Fig. 5a,c). However, if the lengths of the season are unequal (see below) changes in seasonal range will amplify or dampen the effect of season length (e.g, skew).

4.1.3 Change in Relative Season Length

Modifying the relative lengths of the C_3 and C_4 seasons in the seasonal dietary cycle shifts the probability that a random tooth will represent a portion of the C_3 or C_4 season. This manifests in the population of leporid $\delta^{13}C$ values as a change in the relative number of teeth with C_3 or C_4 season $\delta^{13}C$ values. This primarily affects the symmetry of the distribution, which can be seen in changes in skewness and median of the distribution (Fig. 5a,c). When the seasons are of equal length, the distribution is symmetric (skewness of zero) and the median $\delta^{13}C$ value is equal to the annual mean $\delta^{13}C$ value. However, as one season becomes longer than the other, the asymmetry of the distribution increases, leading to increased absolute values of skewness (more negative for a longer C_4 season, and more positive for a longer C_3 season) and a shift in the median towards values typical of the longer season.

The effect of unequal season lengths on skewness and median is amplified by an increase in seasonal vegetation range because the seasonal vegetation range dictates the difference in $\delta^{13}C$ between the two seasons. At larger seasonal ranges, unequal season

lengths will result in the production of longer tails in the tooth $\delta^{13}C$ distribution than at smaller seasonal ranges, resulting in greater absolute skewness in the population. Furthermore, as the seasonal vegetation range increases, the larger differences in the $\delta^{13}C$ values of the seasons make the median of the distribution more sensitive to changes in relative season length.

4.1.4 Inferring Changes in the Seasonal Cycle from Distribution Changes

Though leporid tooth $\delta^{13}C$ distributions can potentially be influenced by each of those types of changes in the seasonal dietary cycle, the degree of control exerted by each type of change varies, resulting in a unique combination of changes in the leporid $\delta^{13}C$ distribution. Each statistic used to describe the synthetic populations is predominantly controlled by one or two types of changes to the seasonal cycle. Skewness can be changed through a shift in seasonal range or mean-state shifts under special circumstances, but the largest changes result from shifts in relative season length. The largest modeled change in skewness due to season length was 1.6, whereas seasonal range can at most result in a shift in skewness of 0.8. Median is potentially susceptible to changes in all three parameters (i.e., relative season length, seasonal range – discussed in 4.1.2 –, and mean state), and as such should be interpreted with caution. In contrast, standard deviation is highly modified by changes in seasonal range ($\leq$ 3.61‰), but shifts in relative season length result in only small changes in the spread of the tooth $\delta^{13}C$ values ($\leq$ 0.74‰). When one season is saturated with one vegetation type (e.g., 100% C_3 or C_4 vegetation), mean-state shifts can change standard deviation as well, but this is through effectively changing the seasonal range.

However, each modeled change in the seasonal dietary cycle does not necessarily occur exclusively. Climate and vegetation dynamics are likely to change in such a way that multiple aspects of the seasonal dietary cycle will shift simultaneously. For example, a decrease in the proportion of C_4 vegetation during solely the C_4 season will be manifested as a change in both seasonal range and mean-state. Cases such as this one, where multiple aspects of changes in the seasonal cycle occur, can result in changes in tooth $\delta^{13}C$ distributions that are difficult to interpret. Changes in median, in particular, can prove to be difficult to interpret because median values are susceptible to both changes in relative season length as well as mean-state shifts. Furthermore, these two changes in the seasonal cycle could occur in such a way that they offset one another's modifications to the median. Such a scenario could arise if a shift in the mean-state towards a greater proportion of C_3 vegetation was coupled with a decrease in the length of the C_3 season. This could be caused by an increase in overall temperature, shortening the C_3 season, combined with a decrease in precipitation during the C_4 growing season, leading to decreased C_4 production and, thus, C_4 plant consumption. The mean-state shift would increase the median leporid $\delta^{13}C$ value, while decreased C_4 season length would decrease the median, offsetting changes in the median due to mean-state shifts.

As a result, discerning changes to the seasonal dietary cycle from changes in leporid $\delta^{13}C$ distributions should rely most heavily on changes in the standard deviation and skewness of the population. Because skewness and standard deviation are predominantly modulated by relative season length and seasonal range, respectively, they provide indicators of these specific types of change to the seasonal cycle. Unambiguous

identification of a shift in the mean vegetation state, however, can be difficult to detect. The median is the only aspect of a leporid $\delta^{13}C$ distribution that reliably changes with mean-state shifts, but changes in relative season length present a possible source of interference. The presence of a mean-state shift is only unambiguous when a change in median is not accompanied by a change in skewness or when median and skewness change in opposite directions from that expected from a change in relative season length.

4.1.5 Error and Testing for Significance

The ability to test whether changes in the median, standard deviation, and skew of the tooth population data are significant is important for assessing whether patterns in the leporid $\delta^{13}C$ distributions are meaningful. The first step in testing for significance is to quantify how well a sample leporid tooth $\delta^{13}C$ distribution approximates aspects of the population from which the sample was drawn. To do so, we used the leporid tooth model presented above to examine the effects of both sample size (i.e., the number of teeth analyzed from a particular interval), and the absolute magnitudes of the changes in seasonal vegetation patterns on the uncertainties in the statistics of the population. This is important in that the number of samples needed to characterize a statistic will differ depending on the magnitude of the vegetation change, the type of change, and the test statistic being used.

In virtually all cases, the median of the population is the most precise statistic for any given sample size. However, the size of the error varies greatly with both seasonal range and relative season length (Fig. 6a). The error is smallest when the combination of seasonal range and relative season length yield populations that have small standard

deviations, high amounts of skewness, or both. The opposite is true for populations with large standard deviations and symmetrical distributions. For example, when there is no seasonal vegetation change, analysis of 10 teeth would yield an error on the median of less than 0.60‰. However, when the seasonal range is maximized (14‰), the error using the same number of teeth increases to 2.65‰. Thus, seasonal range is the primary control on the error in the estimate of the median. Note, however, that at large seasonal vegetation ranges (>10‰), the relative lengths of the seasons can be more important in controlling the error in the median.

Error in the standard deviation behaves in a similar manner to the error in the median, but the errors are larger for a given sample size (Fig. 6b). If there is no seasonal variation in the vegetation (standard deviation = 1.59‰), as few as 25 teeth are needed to achieve an error of 25% (±0.40‰). However, the error in the estimate of standard deviation of the population is positively correlated with the size of the seasonal range. At seasonal ranges greater than 10‰, standard deviation remains positively correlated with seasonal range, but the relative length of the seasons becomes more important, with error minimized in situations where the season lengths are equal.

The error in the estimate of the skewness of the distribution behaves in a manner opposite to that of error of the median, and is the most difficult statistic to quantify. The uncertainty in the estimate of the skew is negatively correlated with the seasonal vegetation range and positively correlated with differences in the lengths of the seasons (Fig. 6c). However, getting precise estimate of the skew is difficult because large numbers of teeth are needed to properly characterize the skewness of a population. For

example, in a situation with large differences in season length (e.g., equivalent to a skew of 0.8), approximately 72 teeth are needed to achieve an error of less than 10% in the estimate of the skew. This lack of precision is likely due to the vulnerability of this statistic to outliers, and, therefore, skewness is not a useful statistic to use in a quantitative fashion unless large numbers of teeth are available. However, as indicated by modeled changes in distribution, it can provide qualitative information about the relative length of the C_3 and C_4 seasons.

These results can be used to compare statistics from two sample distributions and evaluate the statistical significance of the differences between these two distributions. To do this, modeled errors are applied to datasets to estimate the uncertainty prior to application of statistical tests. Because error varies primarily with seasonal vegetation range (Fig. 6), error for a given statistic depends on the seasonal vegetation range of the corresponding distribution. The standard deviation of the distribution is used to estimate the seasonal vegetation range and, consequently, the sets of errors this corresponds to. For a particular statistic, the average of the errors is then applied for use in statistical testing.

The approach used here combines published methods on significance detection (Lanzante, 2005) and the Probability of Detection (P_d) method (Thirumalai et al., pers. comm.) to evaluate whether changes in the sample statistics are significant. The applied threshold for statistical significance, henceforth referred to as the Lanzante Criterion, is

$$|X_1 - X_2| \geq \sqrt{E_1^2 + E_2^2}$$

as described by Lanzante (2005), where X_n refers to a value (median, standard deviation or skewness) with the corresponding errors referred to as E_n.

To estimate the Probability of Detection, a Monte-Carlo-based uncertainty analysis is performed, utilizing the comparison of simulated distributions (n = 10,000) of the statistical parameters (i.e., median, standard deviation, and skew) from each sample derived from the uncertainties in those parameters. All simulated estimates of the statistical parameters from one sample are compared with those from the other sample and tested for significance with the Lanzante Criterion. The Probability of Detection (P_d) is then estimated from the percentage of the pairings that are found to be statistically different. Values that are statistically significantly different from one another will have $P_d \geq 50\%$.

4.2 VARIABILITY ON LONGER TIME SCALES

It is likely, considering the sampling resolution required to obtain sufficient numbers of teeth (at least several hundred to several thousand years), that within individual samples, variability on time scales longer than the seasonal cycle will also play an important role in controlling leporid tooth $\delta^{13}C$ distributions. Variability on longer time scales is capable of producing changes in the median, standard deviation, and skewness of tooth $\delta^{13}C$ distributions similar to those modeled using the seasonal changes in vegetation described above. For example, in a conceptual model of single-foram growth, changes in ENSO variability produce changes in median, skewness, and standard

deviation in a similar manner to that of our modeled changes in the seasonal cycle (Leduc et al., 2009). Although that model only addressed ENSO variability, variability on all time scales can produce similar changes in foram $\delta^{18}O$ distributions. The effect of longer-term variability can play a role in leporid $\delta^{13}C$ distributions as well.

An additional potential complication is the presence of long-term trends in C_3/C_4 vegetation, which can result in the sampling of teeth spanning a change in the seasonal vegetation cycles. Characteristics of the resulting distribution will not be indicative of one population, but will instead be an amalgamation of all the possible seasonal vegetation distributions within the sampled interval. That distorts the values of the statistics used to characterize the distribution. One such example would be sampling across a mean-state shift. Though each year might have a particular seasonal C_3/C_4 range, overlapping multiple years at different mean-states would inflate the $\delta^{13}C$ range in the resulting tooth $\delta^{13}C$ distribution. This leads to a higher standard deviation that would result from just the seasonal dietary cycle. If this were compared to another distribution sampled from an interval with relatively stable vegetation, the change in standard deviation might be interpreted as an increase in the seasonal range, when it is just a product of a long-term shift in vegetation.

The effects of long-term changes in vegetation on leporid $\delta^{13}C$ distributions can be partially mitigated. The most effective strategy for doing so is sampling at high temporal resolution. Because the shape of the leporid $\delta^{13}C$ distribution can only be influenced by variability that occurs within the time frame of the sampling interval, variability on time scales longer than the sampling interval are eliminated as possible

explanatory mechanisms. Ideally, each sampling interval would correspond to a single year, completely eliminating interference from processes occurring above the seasonal level. Though annual resolution is unrealistic, sampling at high resolution helps considerably in limiting the number of sources of variability that can play a role in determining the shape of the resulting leporid $\delta^{13}C$ distributions.

Another consideration is the relative magnitudes of changes in seasonal vegetation versus the changes in vegetation over interannual and longer time scales. When seasonal vegetation changes are much larger than variations that are occurring on longer time scales, seasonal variations in $\delta^{13}C$ values will dominate the distribution of tooth $\delta^{13}C$ values. In most locations with a strong seasonal cycle in vegetation, such as the southwestern United States, this will be the case. A potential exception is when the magnitude of the longer-term variations in $\delta^{13}C$ values approaches the magnitude of the seasonal cycle. In such a scenario, the influence of longer-term variations in vegetation needs to be considered, and will likely be difficult to disentangle from the seasonal cycle. In mid-latitude climates, where there is little seasonality in the proportions of C_3 and C_4 plants, tooth $\delta^{13}C$ distributions will reflect mostly long-term changes in vegetation.

4.3 VARIATIONS IN LEPORID TEETH $\delta^{13}C$ VALUES FROM HALL'S CAVE

To further investigate the utility of leporid tooth $\delta^{13}C$ distributions for reconstructing vegetation change, we used the leporid tooth $\delta^{13}C$ model to investigate changes in tooth $\delta^{13}C$ distributions from Hall's Cave, Texas. Hall's Cave contains a large

number of fossil leporids throughout, partially mitigating the problems associated with interpreting data from small samples. Additionally, the chronology indicates that the Hall's Cave deposit is a product of relatively continuous deposition over the last 20,000 years, during which large shifts in global climate and vegetation occurred over much of North America (e.g., Overpeck et al., 1992). This time span provides the chance to test the sensitivity of the leporid $\delta^{13}C$ record to changes in vegetation.

The bulk organic carbon $\delta^{13}C$ record provides a record of mean C_3/C_4 plant biomass (Table S2). This acts as a baseline to which we can compare the leporid $\delta^{13}C$ record. Long-term shifts in the proportion of C_3/C_4 vegetation on the landscape are evident in the bulk organic $\delta^{13}C$ record, which can be used to divide the bulk carbon record into four distinct vegetation regimes. The first regime, spanning the period between 20 and 14.2 ka BP, is marked by C_4 plant dominance and corresponds to the late Glacial (LG). This is followed by a period of increased C_3 plant abundance from 14 to 11.1 ka. Within the uncertainties in the chronology, this corresponds to the Younger Dryas (YD) event. A third vegetation regime, corresponding to the early Holocene (EH; 11 to 5 ka.) reflects a return to vegetation similar to that of the late Glacial, with C_4 plant dominance. The final vegetation zone, the late Holocene (LH), is marked by a long-term shift towards increased C_3 plant abundance from 5 ka to the present. Leporid teeth were sampled at even spacing throughout each of those vegetation regimes, and replicate teeth were sampled from as many 5 cm excavation levels as possible. The number of teeth sampled for each of these intervals was limited by the number of suitable teeth present in each interval, but allowed for the sampling of 38 teeth in the LH, 35 teeth in the EH, 34

teeth in the YD, and 28 teeth in the late Glacial (Table S1). Given these sample size restrictions, error estimates were made using the statistical criterion described previously (Table 1).

4.3.1 Tooth $\delta^{13}C$ Variability

The leporid tooth $\delta^{13}C$ values exhibit high variability within each interval at Hall's Cave. That variability cannot be explained by the centennial- to millennial-scale C_3/C_4 vegetation variability evident in the bulk organic carbon $\delta^{13}C$ record. The standard deviation of bulk organic $\delta^{13}C$ values is 1.36‰ in the LG, 2.23‰ in the YD, and 1.35‰ in the EH. In contrast, leporid tooth $\delta^{13}C$ variability is greater, with LG, YD, and EH standard deviation values of 1.78‰, 2.97‰, and 2.36‰ during these intervals, respectively. Because each bulk organic carbon $\delta^{13}C$ value integrates vegetation over 59 ±49 years, the spread in $\delta^{13}C$ values will be due to variability on centennial to millennial time scales. These sources of variability influence tooth $\delta^{13}C$ values as well, but since each leporid tooth $\delta^{13}C$ measurement represents 2-4 weeks, the spread in tooth $\delta^{13}C$ values additionally depends on short-term variability, such as decadal, interannual, and seasonal variability. The total variability in leporid $\delta^{13}C$ values is a combination of the variability on these different time scales, while variability in bulk organic $\delta^{13}C$ is the result of only centennial- and millennial-scale variability. Because the variability in tooth $\delta^{13}C$ values is larger than variability of bulk organic $\delta^{13}C$ values, variability on centennial to millennial time scale is not capable of explaining the total variability recorded by the tooth $\delta^{13}C$ record. That means the sub-centennial variability which only the tooth $\delta^{13}C$ values are subject to is providing a noticeable input.

In the LH, however, the long-term shift towards greater C_3 vegetation results in a standard deviation of bulk organic carbon $\delta^{13}C$ values of 2.98‰, compared to the LH standard deviation of tooth $\delta^{13}C$ values of 2.19‰. In this case, centennial and millennial-level variability in mean C_3/C_4 biomass, as reconstructed by the bulk organic $\delta^{13}C$ record, is considerably larger than the variability present in tooth $\delta^{13}C$ values. This means that, in the spread in the LH tooth $\delta^{13}C$ record, the input from the long-term shift in vegetation may be very large, and short-term variability is not necessarily providing substantial input.

The trend of greater variability in tooth $\delta^{13}C$ than in bulk organic $\delta^{13}C$ holds true for replicate teeth sampled from individual excavation levels. Because this sampling interval is 295 ±211 years, variability on this time scale is not subject to millennial-level changes. Comparing variability of the two records at this level permits an assessment of the relative contribution of centennial variability to tooth $\delta^{13}C$ values. For each of the 27 excavation levels from which three teeth were analyzed, excluding those in the LH, the median standard deviation of $\delta^{13}C$ values is 1.69‰ (minimum = 0.41‰, maximum = 4.88‰). However, the median range of bulk organic $\delta^{13}C$ values from the same levels is 1.07‰ (minimum = 0.05‰; maximum = 2.96‰). Similar to the comparison of variability across bins, variability in replicate tooth $\delta^{13}C$ values is larger than bulk organic $\delta^{13}C$ variability. This is evidence that vegetation changes on decadal, interannual, and/or seasonal time scales are increasing tooth $\delta^{13}C$ variability beyond what variability on centennial time scales can produce.

4.3.2 Offset in C_3/C_4 Vegetation

For each interval, tooth $\delta^{13}C$ values indicate lower proportions of C_4 vegetation than evident from the bulk organic $\delta^{13}C$ record, after accounting for isotopic fractionation during production of tooth enamel (Passey et al., 2005). In calculating proportions of C_3/C_4 vegetation from pre-industrial samples, end-member $\delta^{13}C$ values were increased by 1.5‰ to compensate for the decrease in the $\delta^{13}C$ value of atmospheric CO_2 over the last 200 years (Friedli et al., 1986). The bulk organic carbon $\delta^{13}C$ data suggest nearly 100% C_4 plant biomass during the EH and LG, and reconstruct 64% and 78% C_4 plant biomass for the LH and YD, respectively. In contrast, median leporid $\delta^{13}C$ values indicate ca. 25% C_4 plant biomass during the LG, 18% during the YD, 29% during the EH, and 30% during the LH.

Offsets between the median leporid $\delta^{13}C$ values and those estimated from bulk organic carbon $\delta^{13}C$ values beyond that which can be attributed to fractionation may be the result of two processes. First, as discussed previously, dietary bias likely results in some discrepancy between C_3/C_4 plants consumed and C_3/C_4 plants on the landscape, including the preferences for C_3 forbs over C_4 grasses in leporids (Turkowki, 1975; Smith, 2011). Another likely contributor is the limited length of the C_4 growing season. Even when C_4 vegetation dominates total annual C_3/C_4 biomass, C_4 grasses do not grow for the entire year (Correll and Johnston, 1970). Because the $\delta^{13}C$ values of individual teeth represent 2-4 week snapshots of leporid diet, a percentage of $\delta^{13}C$ measurements of randomly sampled teeth will represent portions of the year when C_4 vegetation was not

growing and, therefore, not consumed by leporids. This results in greater representation of C_3 vegetation in leporid $\delta^{13}C$ values than in total C_3/C_4 biomass.

4.3.3 Changes in leporid $\delta^{13}C$ distributions

Errors produced from the model allow for the statistical comparison of tooth $\delta^{13}C$ distributions, which can provide insight into temporal changes in vegetation dynamics. Comparison of the variability in bulk organic carbon $\delta^{13}C$ values to the tooth $\delta^{13}C$ record indicates that short-term variability plays a noticeable role in determining the variability in tooth $\delta^{13}C$ values. Therefore, short-term variability can provide possible explanations for changes in tooth $\delta^{13}C$ distributions. Both the median and standard deviation values were statistically compared between bins; however, skewness was only addressed in a qualitative sense because the sample sizes for each bin are not large enough for a robust quantitative assessment.

4.3.4.1 Late Glacial Variability

The standard deviation of leporid $\delta^{13}C$ values during the LG is significantly lower than during all post-Glacial intervals. At 1.78 ±0.23‰, the standard deviation in $\delta^{13}C$ values during the LG is 40% lower than that during the YD (P_d = 98.3%), 25% lower than that of the EH (P_d = 75.2%), and 19% lower than that of the LH (P_d = 60.1%). As indicated by our model, standard deviation in tooth $\delta^{13}C$ values is positively correlated with the seasonal range in $\delta^{13}C$ values. Thus, the reconstructed increase in the standard deviation in tooth $\delta^{13}C$ values from the LG to the YD and EH may reflect an increase in the seasonal range of C_3/C_4 plant abundance over that time interval, and is consistent with

orbitally induced increases in seasonality over that time period, associated with precession of the equinoxes (Fig. 8a; Berger, 1978).

4.3.4.2 Younger Dryas Variability and Median

The YD leporid tooth $\delta^{13}C$ distribution exhibits the largest standard deviation in the record (2.97‰). Because changes in seasonality modulate changes in the standard deviation of leporid tooth $\delta^{13}C$ distributions, this suggests that the greatest seasonality of C_3/C_4 plant composition in the record occurs during the YD, which cannot be attributed to insolation forcing alone. However, it has been suggested that, in the mid-continent, the YD was characterized by greater temperature seasonality as a result of increased summer advection of warm air masses from the Caribbean (Schiller et al., 1997; Yu and Wright, 2001; Shuman et al., 2002). Because temperature is an important environmental cue for plant life stages (Angevine and Chabot, 1979; Probert, 2000; Volaire and Norton, 2006; Rohde and Bhalerao, 2007), increased seasonality of temperature could result in greater annual extremes in C_3/C_4 vegetation on the landscape, resulting in a greater seasonal range of C_3/C_4 vegetation consumed by leporids.

The increased variability in leporid tooth $\delta^{13}C$ values during the YD is also accompanied by the lowest median $\delta^{13}C$ value (-10.24 ±0.67), 1.02‰ lower than the value for the late Glacial (P_d = 63.9%), 1.62‰ lower than the EH (P_d = 83.5%), and 1.79‰ lower than the LH (P_d = 89.1%). This is consistent with the shift towards greater proportions of C_3 biomass on the landscape apparent in the bulk $\delta^{13}C$ record, though the magnitudes of the changes evident in the tooth and the bulk $\delta^{13}C$ records are significantly different. Alternatively, because relative season length modulates the median of leporid

tooth $\delta^{13}C$ distributions, these changes could have been caused by an increase in the length of the C_3 plant growing season. The peak in skewness during the YD, though not significant, is consistent with this interpretation.

This increase in the length of the C_3 plant growing season during the YD could be due to changes in seasonal precipitation patterns, a decrease in spring and fall temperatures, or a rise in atmospheric pCO_2. Increases in precipitation on either end of the C_3 growing season (i.e., spring and fall) could extend the in C_3 growing season or could allow C_3 winter-annuals to become established earlier in the fall. Because a number of C_3 annuals grow during the spring, increased precipitation during that season could also result in greater amounts of C_3 biomass at this time, effectively extending the C_3 season length, and suppressing the growth and establishment of C_4 summer grasses (Raynal and Bazzaz, 1975; Abul-Fatih and Bazzaz, 1979; Rathcke and Lacey, 1985; Sherry et al., 2008). Likewise, increased precipitation during the fall could allow winter annuals to reach greater biomass earlier in the year, also resulting in a longer C_3 growing season.

Though decreased temperature during from the spring through fall is another possible mechanism for increasing the length of the C_3 growing season, changes in standard deviation support the hypothesis that temperatures were likely more seasonal during the YD. Furthermore, to achieve the observed change in C_3 growing season length compared with the LG would require temperatures to be lower than during the LG, which is unlikely. Thus, it is unlikely that decreased temperature is the primary driver of

changing C_3 growing season length during the YD, though it may be a secondary factor facilitating these changes.

Likewise, changes in atmospheric pCO_2 are capable of changing C_3/C_4 abundance, but are unable to completely explain the patter in the YD. Because C3 plants are favored at higher atmospheric concentrations of CO_2 (Ehleringer et al., 1997), the increase in pCO_2 from the LG to the YD (Petit et al., 1999) could have increased the proportion of the year that favors the growth of C_3 plants. This could explain the decrease in the median of leporid tooth $\delta^{13}C$ values from the LG to the YD. However, this is unable to explain the subsequent increase in median tooth $\delta^{13}C$ values in the EH, where atmospheric CO_2 concentrations were at higher than during the YD (Petit et al., 1999). Instead, the leporid tooth $\delta^{13}C$ data provide strong support for an increase in precipitation during the spring and/or fall seasons and is consistent with the proxy evidence for wetter conditions across the southwestern United States during the YD, likely as a result of a more southerly mean position of the polar front at that time (Asmerom et al., 2010).

4.3.4.3 Lack of Holocene Change

Standard deviation and median values of leporid $\delta^{13}C$ distributions do not undergo significant changes between the EH and LH, when shifts might be expected, based on changes in the bulk organic carbon $\delta^{13}C$ record. LH standard deviation might be expected to have a similar value to the LG because of similar seasonality of insolation. Instead, the standard deviation in tooth $\delta^{13}C$ values is significantly greater during the LH. It is possible that this is the result of confounding influences associated with longer-term

vegetation changes during this time period. Over the late Holocene, bulk organic carbon $\delta^{13}C$ values decrease by ca. 8‰. The magnitude of this change is similar to that of the seasonal cycle, and as a result should have a significant influence on tooth $\delta^{13}C$ values.

Based on this LH decrease in bulk organic carbon $\delta^{13}C$ values, we would expect to see a corresponding decrease in median $\delta^{13}C$ values for leporid teeth. However, this is not apparent in the tooth $\delta^{13}C$ record. One possible explanation for the lack of a change in median leporid $\delta^{13}C$ values is the occurrence of multiple, offsetting changes in the seasonal cycle. For example, the mean-state shift towards more C_3 vegetation would decrease median tooth $\delta^{13}C$ values. That might be offset by a decrease in the relative length of the C_3 season, which, according to our model, should increase the median values of tooth $\delta^{13}C$ values. Such a scenario could be caused by an increase in overall temperature, shortening the C_3 season, combined with a decrease in precipitation during the C_4 growing season, leading to decreased C_4 production and, thus, consumption. The decrease in skewness from the EH to the LH, though not significant, is consistent with this explanation because it indicates a decrease in the relative length of the C_3 season.

An alternative explanation is that some or all of the shift in the LH portion of the bulk organic carbon record occurred in aspects of the vegetation that leporid teeth do not sensitively record. One such case would be if the shift occurred due to changes in vegetation rarely consumed by leporids, such as woody plants. If the LH bulk organic carbon shift was solely due to an increase in the amount of woody vegetation relative to C_4 grasses, it is unlikely that it would be recorded by leporids. An increase in C_3 biomass during the winter is another possible explanation. If leporids already are exclusively

consuming strictly C_3 vegetation during that time of year, a further increase in C_3 biomass will not affect leporid $\delta^{13}C$ values. Additionally, an increase in C_3 biomass during the winter rather than spring or fall would likely leave relative season length unaffected. Given the current data, there is no way to discern which explanation or combination thereof is the most probable.

5 Implications for Interpreting $\delta^{13}C$ values of Small Mammal Teeth

Considering the advantages conferred by small mammal teeth in isotopic studies and their abundance in the fossil record, it is likely that they will continue being used to investigate past changes in vegetation. However, because of their rapid growth, they present a fundamentally different system from those of large mammals, and the differences need to be considered when interpreting stable isotope data from these systems. It is possible to make potentially meaningful interpretations of stable isotope data from small mammal teeth, but this requires a careful consideration of the potential influences of seasonal and longer-term variability on the distribution of tooth isotopic data. However, by using novel approaches, such as characterizing tooth populations from the analysis of large numbers of fast-growing teeth, it is possible to provide additional insights into past variations in vegetation and climate that complement traditional approaches.

Standard deviation, median, and skewness are all aspects of tooth $\delta^{13}C$ distributions that are capable of providing meaningful information about changes in vegetation and climate variability. Provided that the seasonal changes in vegetation are larger than the changes occurring on interannual and longer time scales, the statistics of tooth $\delta^{13}C$ values can be interpreted as reflecting changes in the seasonal cycle. Changes in the median tooth $\delta^{13}C$ values reflect both changes in the mean-state as well as in the relative lengths of the C_3 and C_4 seasons. Variations in the standard deviation of tooth $\delta^{13}C$ distributions provide insights into changes in the magnitude of seasonal changes in

the relative abundance of C_3 and C_4 plants, and changes in the skewness of tooth $\delta^{13}C$ distributions provide an indicator of changes in the relative lengths of the C_3 and C_4 plant growing seasons.

The number of teeth sampled has a significant influence on the ability to properly characterize the tooth population and the ability to distinguish changes in the record. Sampling at small time intervals helps to limit the possible influence of longer-term variability on tooth distributions, but can restrict sample size, which in turn changes the precision of the estimates and the ability to detect meaningful changes. Alternatively, when the sampling interval encompasses a timespan long enough so that the magnitude of non-seasonal $\delta^{13}C$ variations approach seasonal changes in $\delta^{13}C$, these two effects cannot be separated, and the interpretation of the $\delta^{13}C$ data is more ambiguous.

The model generated here specifically focused on leporids – which are abundant in Hall's Cave and across the Edwards Plateau. The stable isotope values in teeth of other taxa with different ecologies and physiologies will potentially reflect changes in vegetation differently. Many rodents, for example, do not have hypselodont cheek teeth (Ungar, 2010), and if this is paired with a distinct breeding season, each tooth might reflect a specific part of the year, creating a bias in the interpretation of the vegetation data. A similar complication applies to hibernating mammals. Animals that store their food are likely to sample the vegetation differently and might not alter their diet seasonally. Other such behaviors and physiological considerations need to be taken into account when interpreting these data. Modeling approaches, like the one presented here,

provide an interpretive framework for understanding the data generated from these kinds of systems.

6 Figures and Tables

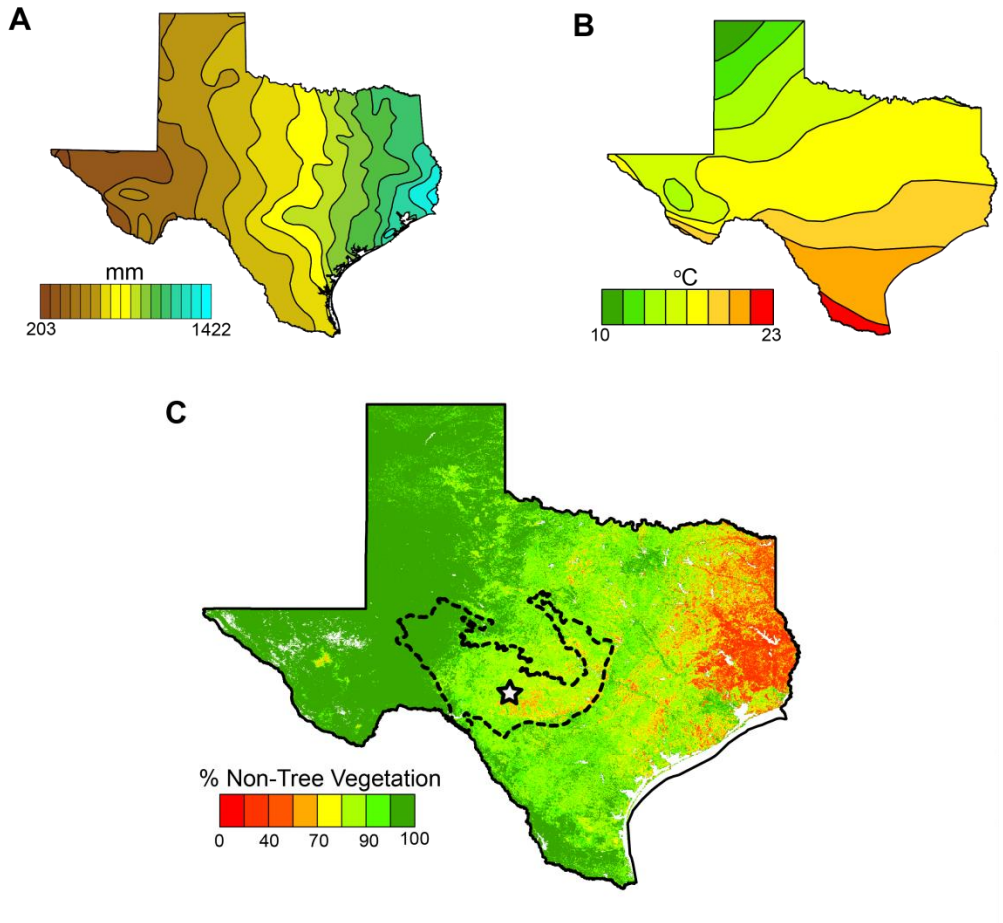

Figure 1: Modern climate and vegetation of Texas. (**A**) Modern mean annual precipitation in millimeters adapted from the Texas Parks and Wildlife Department. (**B**) Modern mean annual temperature as interpolated from data provided by NOAA. (**C**) Percentage of the vegetation that is not trees. Bare ground and water features are white. The star marks the location of Hall's Cave, and the dashed line denotes the boundary of the Edwards Plateau as recognized by the Texas Parks and Wildlife Department. Percentage of non-tree vegetation was calculated from MODIS Vegetation Continuous Fields collection 5 (DiMiceli et al., 2011).

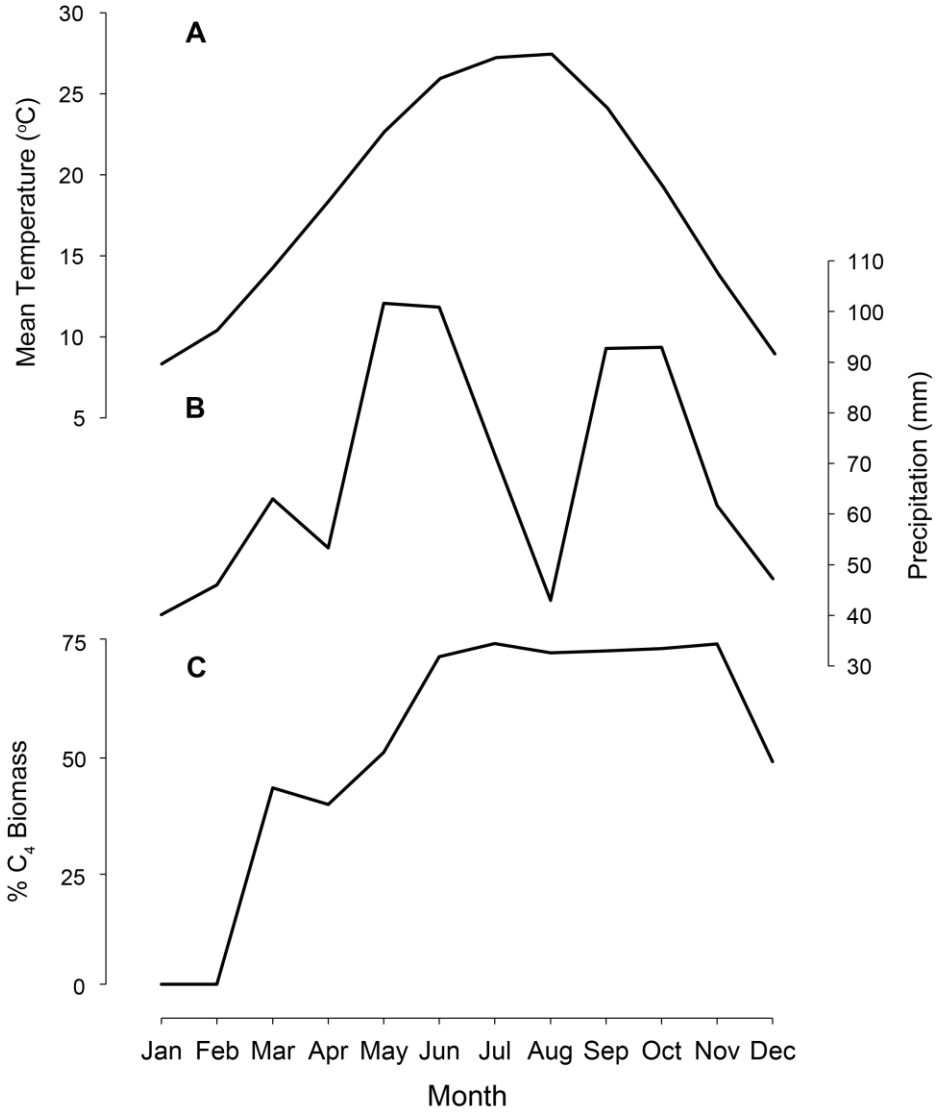

Figure 2: Modern seasonal climate and vegetation of the study area. Mean monthly temperature (**A**) and mean monthly precipitation (**B**) are averages from 1981-2010 at the Kerrville 3 NNE weather station (30°4'28"N 99°6'31"W). Data were collected from the National Climate Data Center (www.ncdc.noaa.gov). Monthly changes in % C_4 biomass (**C**) are for sites west of the Balcones Escarpment in Travis, Hays, and Blanco Counties. Relative abundances were calculated using relative abundance data from Fowler and Dunlap (1986) and growing season data from Correll and Johnston (1970).

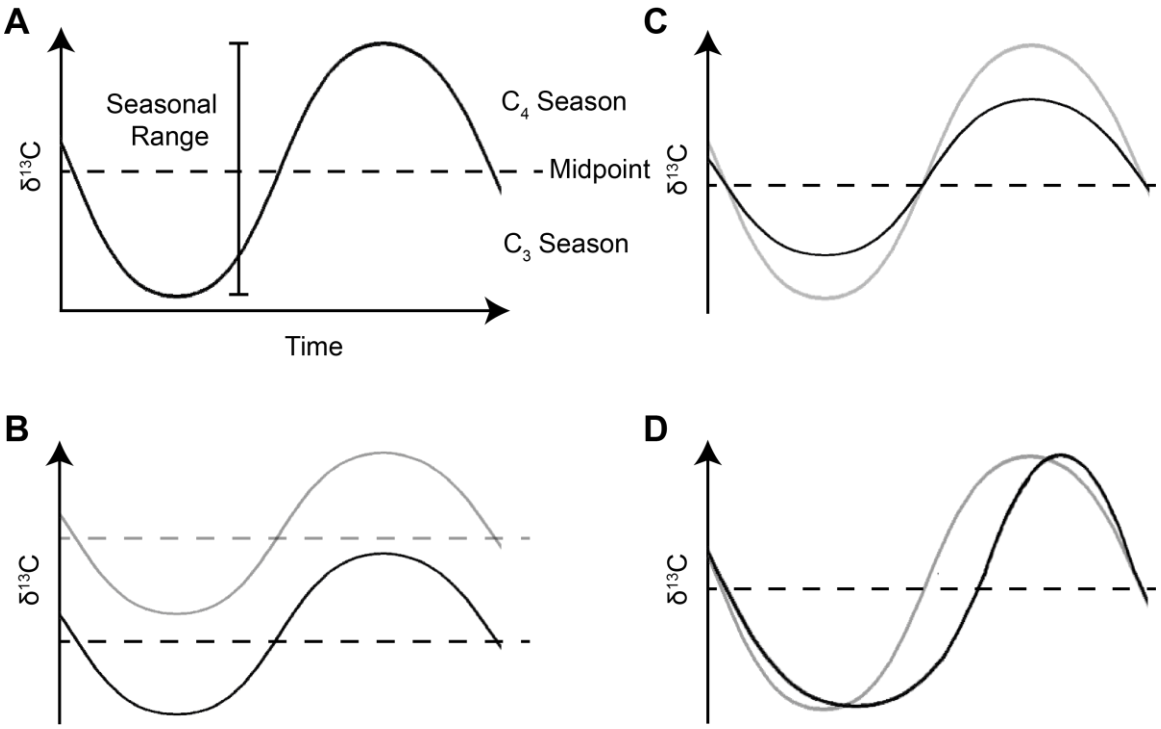

Figure 3: Anatomy of and possible changes to intra-annual changes in vegetation. (**A**) Terminology used to refer to parts of our model of intra-annual vegetation change. (**B**, **C**, **D**) Illustrations of the effect of mean-state shift, change in amplitude, and change in relative season length, respectively.

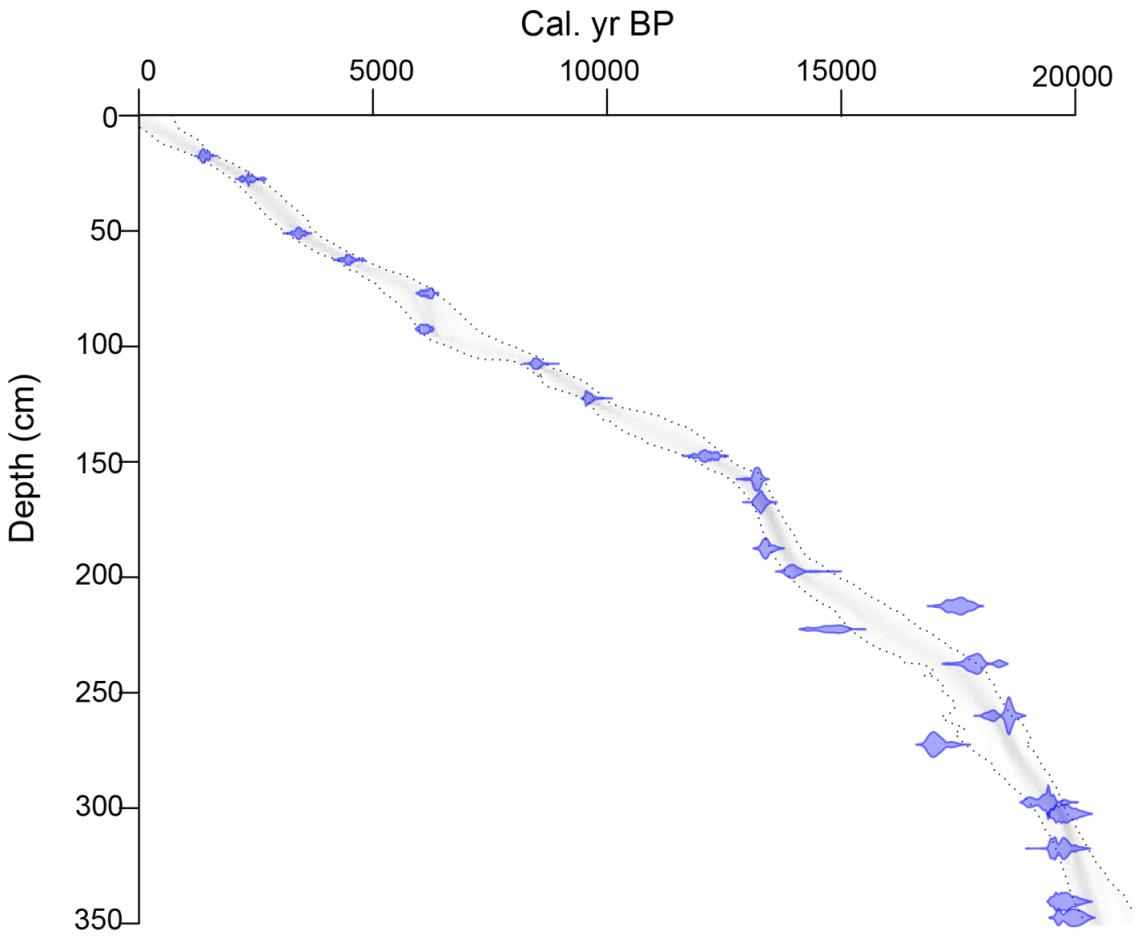

Figure 4: Age model of Hall's Cave deposit. Probability distributions for the calibration of individual radiocarbon dates are indicated, with thicker portions indicating higher probability of correspondence to that age. Dotted lines indicate 95% probability intervals. Darker shaded areas indicate a greater number of replications. To generate the age model, we used the R-script BACON (Blaauw and Christen, 2011) with a mean accumulation rate of 52 years/cm, a 5 cm sampling window size, and a sample size of 10,000.

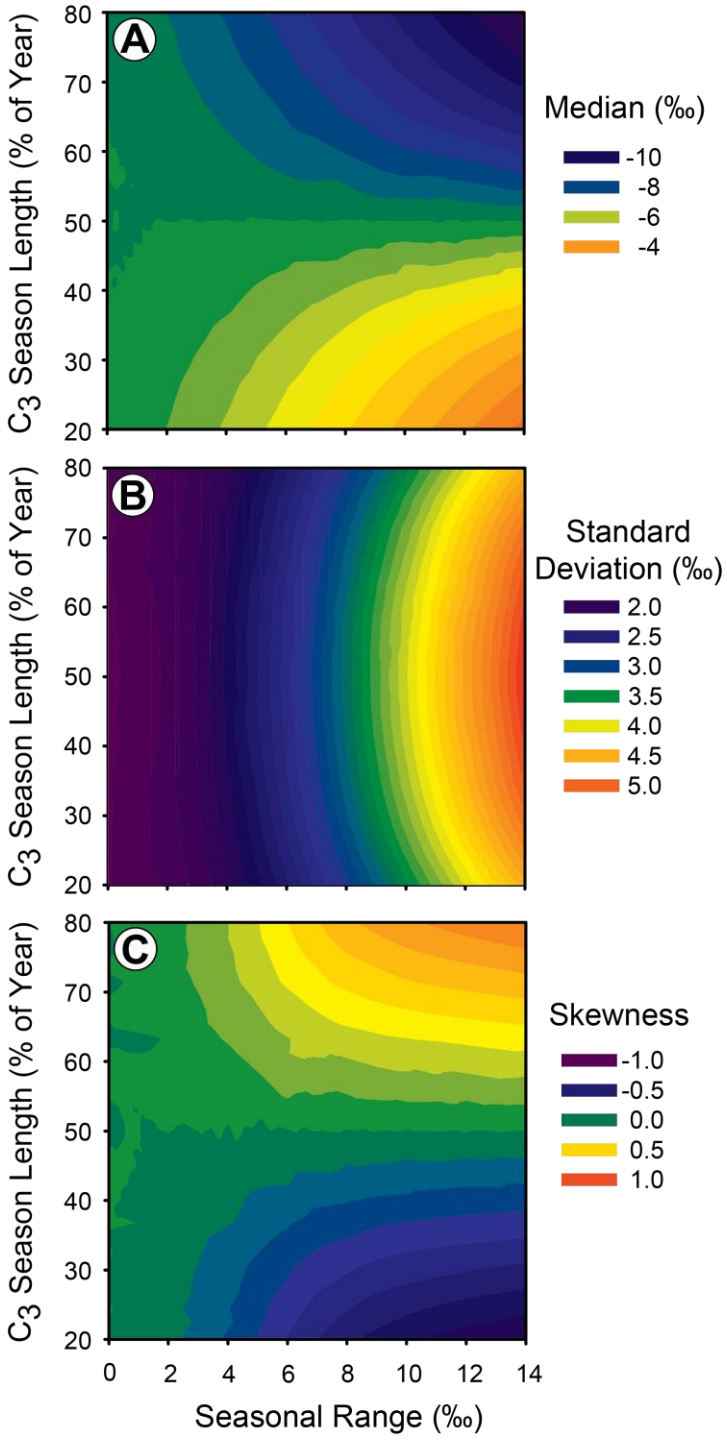

Figure 5: Contour plots representing changes in median (**A**), standard deviation (**B**), and skewness (**C**) as a function of C_3 season length and amplitude. For all plots, we set the resting position to 50% C_3 and used synthetic populations of 100,000 teeth in the creation of the plots.

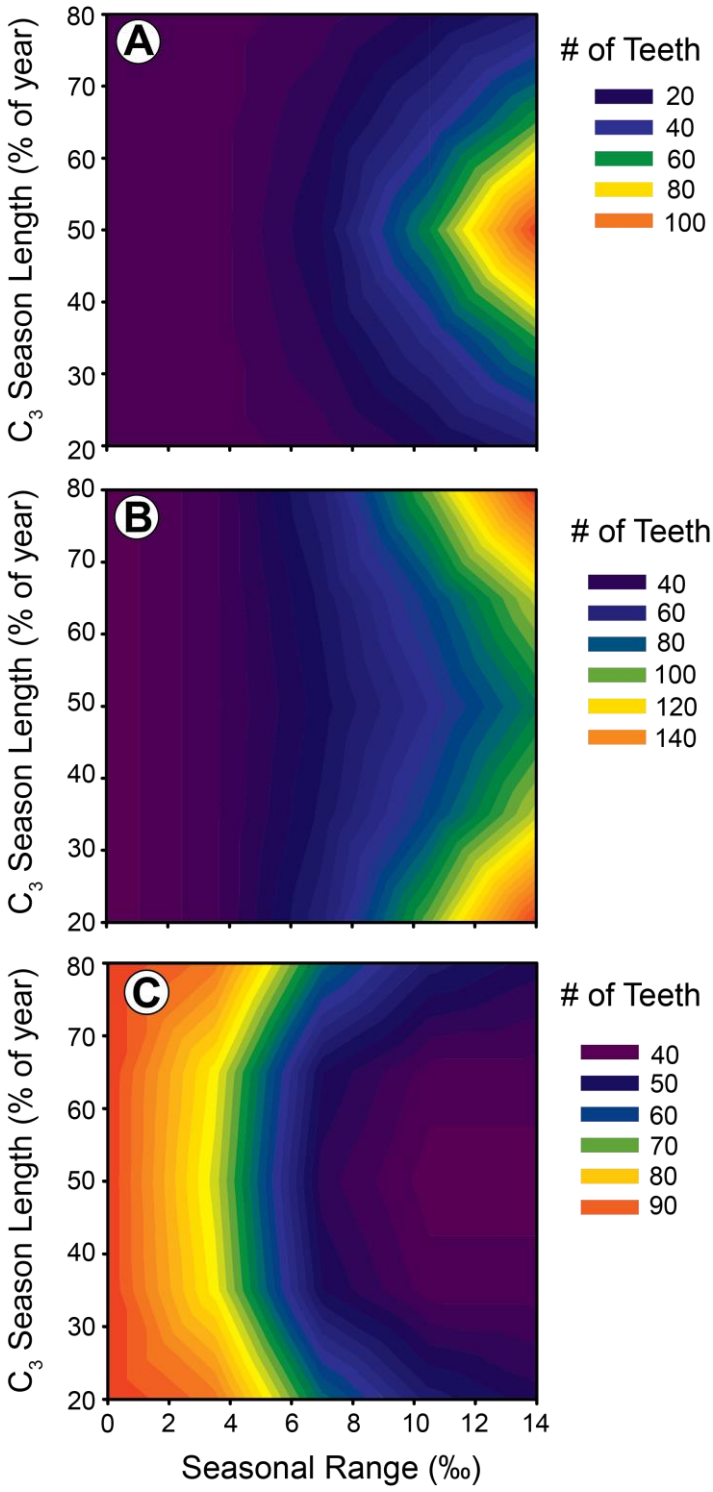
A
B
C
C_3 Season Length (% of year)
Seasonal Range (‰)
# of Teeth
20
40
60
80
100
120
140
50
70
90
0
2
4
6
8
10
12
14
20
30
40
50
60
70
80

Figure 6: Sample size requirements. (**A**) The number of teeth required for the error of the median to reach 1‰. Median is best estimated when standard deviations are small and the distribution is symmetric because those scenarios present cluster the middle values around a small range of $\delta^{13}C$ values. (**B**) The number of teeth required for the error of the standard deviation to reach 0.25‰. Standard deviation requires more teeth to estimate high variances because under- or overrepresentation of the tails result in a greater difference in $\delta^{13}C$ values. Very skewed distributions also require more teeth because the long tail represents few teeth but make a large contribution to variance. (**C**) The number of teeth required for the error of skewness to reach 0.25. As seasonal range decreases or skewness increases, the distribution becomes more peaked, increasing the $\delta^{13}C$ range of the tails relative to the rest of the distribution. This makes skewness more difficult to estimate. Each is plotted as a function of amplitude and C_3 season length. 10,000 realizations of each sample size were used in error calculation.

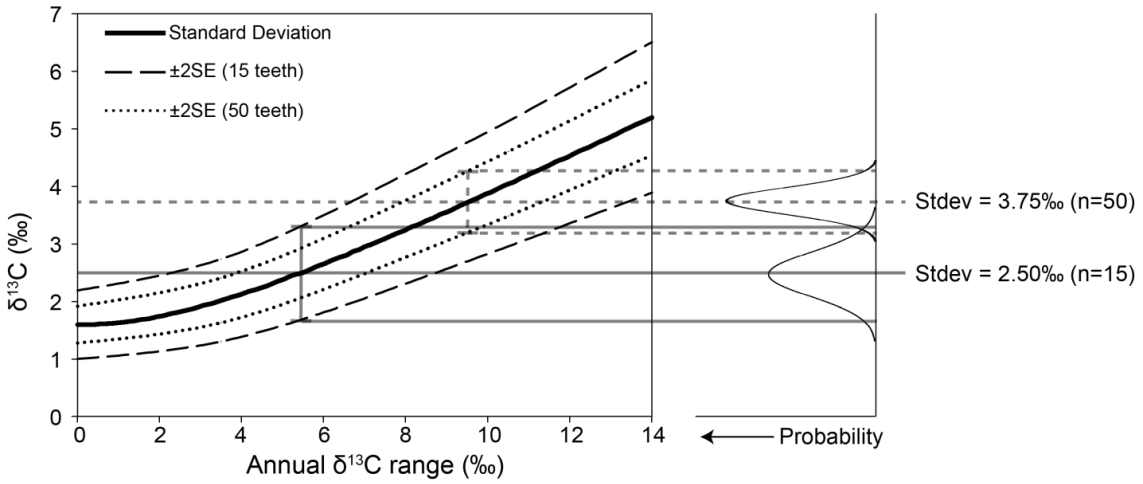

Figure 7: Illustration of how errors are applied to standard deviation using hypothetical datasets indicated on the far right. The depicted relationship between $\delta^{13}C$ range and standard deviation is for a model with C_3 and C_4 seasons of equal length.

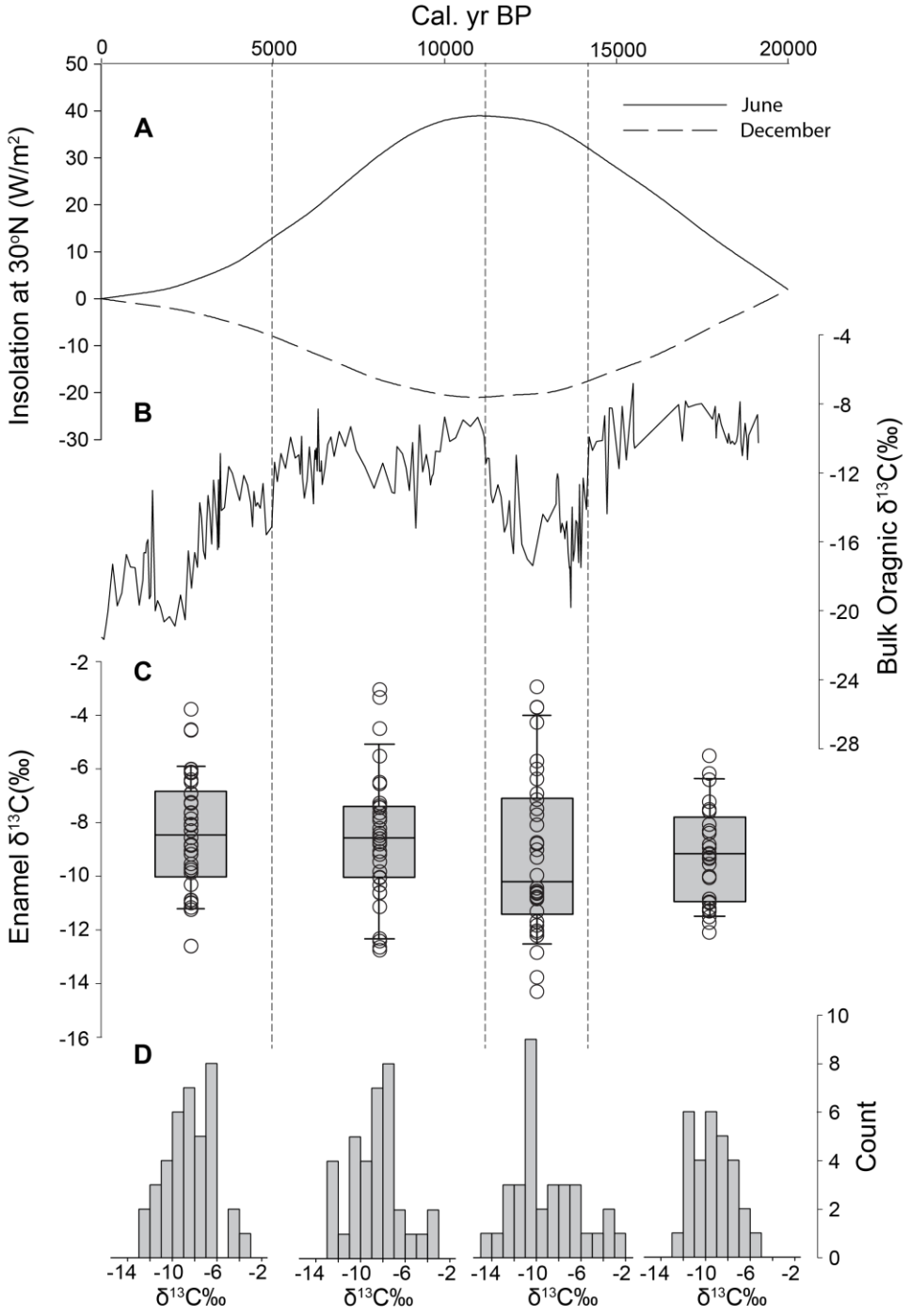

	Late Holocene	Early Holocene	Younger Dryas	Glacial
Age Range (Cal. yr BP)	0-5000	5000-11000	11100-14000	14200-20000
Sample Size	38	35	34	29
Standard Deviation	2.19±0.25‰	2.36±0.25‰	2.97±0.31‰	1.78±0.23‰
Median	-8.45±0.46‰	-8.62±0.48‰	-10.24±0.67‰	-9.22±0.40‰

Figure 8: Summary of enamel carbon isotope measurements. (**A**) Changes in seasonal insolation at 30^{o}N over the last 20,000 years (Berger, 1978). (**B**) Bulk organic stable carbon isotope record. (**C**) δ^{13}C values for individual teeth plotted (open circles) on top of corresponding 10-90th percentile box plots. Each set of teeth are plotted at their mean age, but individual teeth were sampled from various ages scattered throughout each interval. (**D**) Histograms of tooth isotope values from each interval with summary statistics below. Dotted lines on **A** – **C** indicate temporal boundaries between leporid tooth δ^{13}C distributions.

	LH-EH	LH-YD	LH-G	EH-YD	EH-G	YD-G
SD	-	88.6	60.1	77.2	75.2	98.3
Median	-	89.1	61.7	83.5	-	63.9

Table 1: Probabilities of detection. Column headings indicate the intervals compared. Probabilities are only shown for pairs that are statistically significant according to the criterion detailed by Lanzante (2005).

7 Appendices

APPENDIX A: SUPPLEMENTAL TABLES

Table S1: Leporid tooth $\delta^{13}C$ values. All isotope values are reported relative to VPDB. Age is that of the midpoint of the depth interval the tooth came from.

Specimen Number	Pit	Depth (cm)	Tooth	Side	$\delta^{13}C$ (‰)	$\delta^{13}C$ stdev (‰)	$\delta^{18}O$ (‰)	$\delta^{18}O$ stdev (‰)	Age (Cal. yr BP)
TMM 41229-13130	1a	0-5	upper P4 or M1	right	-4.58	0.011	-1.03	0.026	105.25
TMM 41229-13134	1a	0-5	upper P4 or M1	right	-9.07	0.011	-0.03	0.021	105.25
TMM 41229-13135	1a	0-5	upper P3	right	-4.56	0.013	0.97	0.036	105.25
TMM 41229-13143	1	5-10	upper M2	left	-8.86	0.022	-1.05	0.086	652.75
TMM 41229-13144	1a	5-10	upper P4 or M1	left	-7.65	0.013	0.05	0.022	652.75
TMM 41229-13145	1	5-10	upper P4 or M1	right	-6.42	0.023	-0.41	0.021	652.75
TMM 41229-13146	1e	10-15	upper P3	left	-12.62	0.011	-4.36	0.022	1212.85
TMM 41229-13147	1b	10-15	upper P3	left	-3.80	0.017	0.42	0.023	1212.85
TMM 41229-4836	1	10-15	upper P4 or M1	left	-10.34	0.011	-1.66	0.028	1212.85
TMM 41229-13148	1	15-20	upper P4 or M1	left	-11.02	0.018	0.16	0.032	1359
TMM 41229-13149	1a	15-20	upper M2	left	-7.31	0.014	-0.42	0.028	1359
TMM 41229-13150	1a	15-20	upper P4 or M1	right	-12.62	0.013	-1.65	0.041	1359
TMM 41229-13151	1e	20-25	upper M2	left	-6.03	0.019	-1.92	0.025	1649.5
TMM 41229-13152	1e	20-25	upper P4 or M1	left	-9.71	0.011	0.13	0.027	1649.5
TMM 41229-13153	1e	20-25	upper P4 or M1	right	-6.04	0.014	-2.54	0.023	1649.5
TMM 41229-13154	1e	25-30	upper P4 or M1	left	-7.66	0.011	2.17	0.021	2305.5
TMM 41229-13155	1e	25-30	lower P4, M1, or M2	right	-8.58	0.010	0.48	0.017	2305.5
TMM 41229-13156	1c	25-30	upper M2	left	-8.12	0.011	3.85	0.028	2305.5
TMM 41229-13157	1a	30-35	upper M2	left	-6.93	0.011	-1.87	0.037	2788.35

Table S1 (continued)

Specimen Number	Pit	Depth (cm)	Tooth	Side	$\delta^{13}C$ (‰)	$\delta^{13}C$ stdev (‰)	$\delta^{18}O$ (‰)	$\delta^{18}O$ stdev (‰)	Age (Cal. yr BP)
TMM 41229-13158	1a	30-35	upper P3	right	-7.26	0.016	1.19	0.023	2788.35
TMM 41229-13159	1a	30-35	upper P4, M1 or M2	right	-6.13	0.018	-0.59	0.019	2788.35
TMM 41229-13160	1	35-40	upper M2	left	-9.78	0.018	-0.13	0.047	3054.6
TMM 41229-13161	1a	35-40	upper M2	right	-11.27	0.012	-0.63	0.030	3054.6
TMM 41229-13162	1	40-45	upper P3	right	-7.88	0.007	0.19	0.012	3292.6
TMM 41229-13163	1e	45-50	upper P4 or M1	right	-8.84	0.009	0.52	0.016	3429.6
TMM 41229-13164	1e	45-50	upper P4 or M1	right	-11.00	0.003	2.42	0.012	3429.6
TMM 41229-13165	1e	45-50	upper P4 or M1	right	-11.19	0.011	-1.09	0.025	3429.6
TMM 41229-13131	1	50-55	possibly upper M1	right	-8.88	0.018	0.92	0.027	3536.4
TMM 41229-13136	1	50-55	possibly upper P4	left	-10.90	0.013	0.33	0.029	3536.4
TMM 41229-13137	1	50-55	possibly upper P4	right	-8.09	0.012	1.74	0.019	3536.4
TMM 41229-13167	1e	55-60	upper P4 or M1	left	-6.17	0.006	0.17	0.018	4074.4
TMM 41229-13168	1e	55-60	upper P3	right	-9.56	0.019	-0.53	0.032	4074.4
TMM 41229-13169	1e	60-65	upper P4 or M1	left	-8.32	0.014	-0.18	0.049	4452.5
TMM 41229-13170	1e	60-65	upper P4 or M1	left	-6.51	0.018	-1.31	0.036	4452.5
TMM 41229-13171	1e	60-65	upper P4 or M1	right	-9.20	0.009	-2.04	0.035	4452.5
TMM 41229-13172	1d	65-70	upper P4 or M1	right	-10.92	0.016	-3.77	0.033	4813.05
TMM 41229-13173	1d	65-70	upper M2	left	-6.95	0.014	2.12	0.034	4813.05
TMM 41229-13174	1d	65-70	upper P4 or M1	right	-9.89	0.022	-1.97	0.018	4813.05
TMM 41229-13176	1d	70-75	upper P3	left	-7.38	0.012	1.32	0.023	5236.85
TMM 41229-13177	1	70-75	upper P4 or M1	left	-9.85	0.007	-0.26	0.013	5236.85
TMM 41229-13178	1b	75-80	upper P3	left	-7.95	0.023	1.05	0.033	5776.3
TMM 41229-13179	1b	75-80	upper P4 or M1	left	-8.24	0.023	3.11	0.021	5776.3
TMM 41229-13180	1a	75-80	upper P4 or M1	right	-7.30	0.014	-1.69	0.016	5776.3
TMM 41229-13181	1d	80-85	upper P4 or M1	right	-12.66	0.013	-1.95	0.032	6043.6

Table S1 (continued)

Specimen Number	Pit	Depth (cm)	Tooth	Side	$\delta^{13}C$ (‰)	$\delta^{13}C$ stdev (‰)	$\delta^{18}O$ (‰)	$\delta^{18}O$ stdev (‰)	Age (Cal. yr BP)
TMM 41229-13182	1d	80-85	upper P4 or M1	right	-7.83	0.009	2.09	0.037	6043.6
TMM 41229-13183	1d	80-85	upper P4 or M1	right	-4.51	0.014	3.21	0.046	6043.6
TMM 41229-13184	1d	85-90	upper P3	right	-7.82	0.010	-1.64	0.026	6216.6
TMM 41229-13185	1d	85-90	upper P4 or M1	left	-9.48	0.015	-1.84	0.027	6216.6
TMM 41229-13186	1d	85-90	upper M2	left	-8.74	0.010	-2.11	0.029	6216.6
TMM 41229-13187	1d	90-95	upper P4 or M1	left	-8.51	0.015	-2.33	0.021	6338.5
TMM 41229-13188	1d	90-95	upper P4 or M1	left	-6.52	0.017	1.24	0.032	6338.5
TMM 41229-13189	1d	90-95	upper P4 or M1	left	-9.10	0.021	2.42	0.064	6338.5
TMM 41229-13190	1d	95-100	upper P4 or M1	right	-10.06	0.020	-0.75	0.011	6556.85
TMM 41229-13191	1d	95-100	upper P3	left	-8.82	0.014	0.18	0.034	6556.85
TMM 41229-13192	1d	95-100	upper P3	left	-10.34	0.008	-2.72	0.023	6556.85
TMM 41229-13132	1d	100-105	upper P4 or M1	left	-8.63	0.013	-0.41	0.056	7176.15
TMM 41229-13138	1d	100-105	upper P4 or M1	right	-9.21	0.010	-1.00	0.025	7176.15
TMM 41229-13139	1d	100-105	broken upper cheek tooth	left	-3.36	0.012	2.26	0.030	7176.15
TMM 41229-13193	1d	105-110	upper M2	left	-7.47	0.017	2.60	0.027	8309.55
TMM 41229-13194	1d	105-110	upper cheek tooth	right	-12.35	0.013	-0.19	0.021	8309.55
TMM 41229-13195	1d	105-110	upper M2	right	-11.16	0.018	-0.36	0.026	8309.55
TMM 41229-13196	1d	110-115	broken upper cheek tooth	left	-5.54	0.008	1.02	0.023	8792.55
TMM 41229-13197	1d	110-115	upper P4 or M1	left	-6.58	0.007	-1.07	0.017	8792.55
TMM 41229-13198	1b	110-115	upper P4, M1, or M2	right	-10.63	0.010	-1.71	0.018	8792.55
TMM 41229-13199	1d	115-120	upper P4 or M1	left	-12.77	0.016	1.83	0.027	9269.8
TMM 41229-13200	1d	115-120	upper P4 or M1	left	-8.62	0.012	-2.01	0.025	9269.8
TMM 41229-13201	1d	115-120	upper P4 or M1	right	-10.62	0.016	2.11	0.028	9269.8
TMM 41229-13202	1	120-125	upper P3	left	-8.41	0.013	2.88	0.030	9607.6
TMM 41229-13203	1	120-125	upper M2	right	-7.45	0.010	-2.24	0.021	9607.6

Table S1 (continued)

Specimen Number	Pit	Depth (cm)	Tooth	Side	$\delta^{13}C$ (‰)	$\delta^{13}C$ stdev (‰)	$\delta^{18}O$ (‰)	$\delta^{18}O$ stdev (‰)	Age (Cal. yr BP)
TMM 41229-13204	1	120-125	upper P4 or M1	left	-7.66	0.011	0.10	0.033	9607.6
TMM 41229-13205	1d	125-130	upper P4 or M1	right	-12.44	0.005	0.89	0.036	10136.75
TMM 41229-13206	1d	125-130	upper P3	right	-10.08	0.016	-3.08	0.034	10136.75
TMM 41229-13207	1d	125-130	upper P3	left	-3.06	0.013	5.14	0.022	10136.75
TMM 41229-13208	1d	130-135	upper P4 or M1	right	-10.00	0.012	-2.69	0.014	11077.95
TMM 41229-13209	1d	130-135	upper P3	right	-8.12	0.015	0.42	0.025	11077.95
TMM 41229-13210	1d	130-135	upper P4 or M1	left	-4.31	0.016	1.57	0.032	11077.95
TMM 41229-13211	1e	135-140	upper P4 or M1	left	-8.78	0.013	1.47	0.038	11312.1
TMM 41229-13212	1e	135-140	upper P3, P4, or M1	right	-10.82	0.018	-0.98	0.020	11312.1
TMM 41229-13213	1e	135-140	upper P4 or M1	right	-12.14	0.010	-1.10	0.016	11312.1
TMM 41229-13214	1e	140-145	upper P4 or M1	right	-10.58	0.020	3.00	0.031	11657.7
TMM 41229-13215	1e	140-145	upper P4 or M1	left	-10.68	0.010	-1.54	0.034	11657.7
TMM 41229-13216	1e	140-145	upper P4 or M1	right	-11.35	0.012	-0.95	0.021	11657.7
TMM 41229-13133	1e	145-150	upper P4 or M1	left	-8.83	0.015	-1.78	0.023	11981.25
TMM 41229-13140	1e	145-150	upper P4 or M1	left	-3.74	0.015	4.43	0.028	11981.25
TMM 41229-13141	1e	145-150	upper P4 or M1	right	-12.06	0.018	0.58	0.031	11981.25
TMM 41229-13217	1d	152-155	upper P4 or M1	left	-7.52	0.016	-2.12	0.021	12651.55
TMM 41229-13218	1d	152-155	upper P4 or M1	left	-10.88	0.025	-0.13	0.029	12651.55
TMM 41229-13219	1d	152-155	upper P3	left	-6.04	0.018	-0.69	0.022	12651.55
TMM 41229-13220	1d	155-160	upper P4 or M1	right	-10.48	0.009	-6.39	0.028	12899.75
TMM 41229-13221	1d	155-160	upper P4 or M1	right	-11.73	0.013	-3.41	0.025	12899.75
TMM 41229-13222	1d	155-160	upper P3	right	-10.64	0.013	-5.73	0.027	12899.75
TMM 41229-13223	1e	160-165	upper P4 or M1	left	-10.79	0.010	-4.52	0.019	13231.6
TMM 41229-13224	1e	160-165	upper M1 or M2	left	-9.05	0.017	-3.91	0.032	13231.6
TMM 41229-13225	1e	160-165	upper P4 or M1	right	-9.33	0.009	-5.47	0.015	13231.6

Table S1 (continued)

Specimen Number	Pit	Depth (cm)	Tooth	Side	$\delta^{13}C$ (‰)	$\delta^{13}C$ stdev (‰)	$\delta^{18}O$ (‰)	$\delta^{18}O$ stdev (‰)	Age (Cal. yr BP)
TMM 41229-13226	1e	165-170	upper M2	left	-10.81	0.013	-3.63	0.044	13385.3
TMM 41229-13227	1e	165-170	upper P4 or M1	right	-3.73	0.010	0.84	0.016	13385.3
TMM 41229-13228	1e	165-170	upper M2	left	-5.74	0.009	-0.02	0.028	13385.3
TMM 41229-13229	1e	170-175	upper M2	left	-12.25	0.014	-0.87	0.019	13435.9
TMM 41229-13230	1e	170-175	upper P3	left	-7.75	0.017	-1.83	0.042	13435.9
TMM 41229-13231	1e	170-175	upper P4 or M1	left	-6.95	0.018	-0.65	0.028	13435.9
TMM 41229-13232	1d/e	175-180	upper P3	right	-14.33	0.016	-3.16	0.025	13524.1
TMM 41229-13233	1d/e	175-180	upper P4 or M1	left	-12.87	0.014	-3.21	0.020	13524.1
TMM 41229-13234	1d/e	175-180	upper M2	right	-13.80	0.012	-3.54	0.020	13524.1
TMM 41229-13235	1e	180-185	upper P3	left	-7.18	0.013	-1.73	0.023	13654.45
TMM 41229-13236	1e	180-185	upper M2	left	-2.98	0.018	-1.90	0.033	13654.45
TMM 41229-13237	1c	180-185	upper P4 or M1	right	-11.87	0.008	-2.84	0.012	13654.45
TMM 41229-13239	1c	190-195	broken upper cheek tooth	right	-6.41	0.013	-2.58	0.019	13998.65
TMM 41229-5223	1c	195-200	upper P4 or M1	right	-11.76	0.014	-3.73	0.024	14319.55
TMM 41229-4780	1c	200-205	upper P3	left	-6.20	0.012	-1.80	0.012	14479.5
TMM 41229-13142	1b	200-205	upper P4 or M1	right	-6.44	0.006	2.37	0.022	14479.5
TMM 41229-4782	1c	200-205	lower P4, M1, or M2	right	-8.85	0.011	-3.05	0.017	14479.5
TMM 41229-13240	1c	205-210	upper P4 or M1	right	-8.11	0.012	-1.23	0.038	14766.25
TMM 41229-13241	1d/e	210-215	upper M2	right	-11.34	0.008	-3.70	0.023	15202.6
TMM 41229-13242	1d/e	210-215	upper P4 or M1	left	-10.09	0.014	-2.19	0.026	15202.6
TMM 41229-13243	1d/e	210-215	upper P4 or M1	left	-9.22	0.016	0.71	0.023	15202.6
TMM 41229-13244	1d/e	215-220	upper P4 or M1	left	-7.62	0.016	-1.04	0.017	15406.2
TMM 41229-13245	1d/e	215-220	upper P3	left	-5.55	0.016	-1.19	0.027	15406.2
TMM 41229-13246	1d/e	220-225	upper P4 or M1	right	-9.58	0.016	-1.26	0.031	15708.65
TMM 41229-13247	1d/e	220-225	upper P3	right	-9.33	0.009	-1.83	0.032	15708.65

Table S1 (continued)

Specimen Number	Pit	Depth (cm)	Tooth	Side	$\delta^{13}C$ (‰)	$\delta^{13}C$ stdev (‰)	$\delta^{18}O$ (‰)	$\delta^{18}O$ stdev (‰)	Age (Cal. yr BP)
TMM 41229-13248	1d/e	220-225	upper P4 or M1	left	-7.55	0.010	-0.72	0.021	15708.65
TMM 41229-13249	1d/e	225-230	upper M2	right	-11.55	0.017	-0.45	0.019	15919.6
TMM 41229-13250	1d/e	225-230	upper P4 or M1	left	-9.38	0.017	-1.91	0.024	15919.6
TMM 41229-13251	1d/e	225-230	upper P4 or M1	right	-12.13	0.011	-0.83	0.027	15919.6
TMM 41229-13252	1d/e	230-235	upper P4 or M1	right	-10.99	0.016	-1.70	0.035	16144.35
TMM 41229-13253	1d/e	230-235	upper P3	left	-7.26	0.009	-0.13	0.018	16144.35
TMM 41229-13254	1d/e	230-235	upper P3	right	-10.88	0.011	-4.35	0.030	16144.35
TMM 41229-13255	d	235-240	upper P4 or M1	left	-11.31	0.013	-4.07	0.019	16769.75
TMM 41229-13256	d	240-245	upper P4 or M1	left	-10.03	0.016	-3.41	0.025	17139.9
TMM 41229-13257	d	245-250	upper P4 or M1	left	-11.22	0.016	-1.35	0.036	17758
TMM 41229-13264	d	250-255	upper P4 or M1	right	-9.18	0.012	-1.75	0.035	17948.95
TMM 41229-13258	1d	255-260	upper P4 or M1	right	-8.42	0.013	-1.18	0.030	18214.65
TMM 41229-13262	d	260-265	upper P3	right	-7.61	0.022	1.37	0.041	18400.25
TMM 41229-13263	d	260-265	upper P4 or M1	right	-8.34	0.017	1.71	0.027	18400.25
TMM 41229-13259	1d	280-285	upper P4 or M1	right	-8.97	0.013	-0.86	0.033	18971.55
TMM 41229-13260	1d	285-290	upper P4 or M1	left	-11.03	0.012	-2.90	0.018	19150.05
TMM 41229-13261	1e	295-300	upper M2	right	-9.18	0.023	-2.05	0.033	19571.45

Table S2: Bulk organic carbon isotope data. Carbon isotope values are reported relative to VPDB. $\%C_4$ is calculated using C_3 and C_4 end-members of -27‰ and -13‰, respectively.

Depth (cm)	Corrected Depth (cm)	%C	$\delta^{13}C$ (‰)	$\%C_4$	Age (Cal. yr bp)
0-1	-7.26285	0.070544	-18.6991	0.592922	-48.2685
1-2	-6.24275	0.076682	-20.3999	0.471436	-47.5285
2-3	-5.22265	0.077705	-18.5713	0.602051	-46.7885
3-4	-4.20255	0.070889	-20.3958	0.471726	-46.0485
4-5	-3.18245	0.064934	-19.751	0.517782	-45.3085
5-6	-2.16235	0.081728	-20.267	0.480926	-44.5686
6-7	-1.14225	0.085622	-21.5933	0.386193	-43.8286
7-8	-0.12215	0.074729	-21.441	0.397068	-43.0886
8-9	0.89795	0.072134	-21.437	0.397357	10.24844
9-10	1.91805	0.063991	-21.5578	0.388731	70.74037
10-11	2.93815	0.079427	-20.6818	0.451297	131.2323
11-12	3.95825	0.06677	-19.9134	0.506189	191.6284
12-13	4.97835	0.06141	-17.2191	0.698638	322.3617
13-14	5.99845	0.063249	-19.6364	0.525975	455.997
14-15	7.01855	0.061751	-18.8913	0.579193	589.6319
15-16	8.03865	0.074992	-16.6793	0.737194	722.9612
16-17	9.05875	0.066958	-17.3915	0.68632	845.9853
17-18	10.07885	0.06817	-17.4313	0.683477	969.0093
18-19	11.09895	0.070968	-19.5865	0.529535	1092.033
19-20	12.11905	0.06066	-18.1372	0.633056	1203.593
20-21	13.13915	0.060526	-16.596	0.743143	1228.367
21-22	14.15925	0.054659	-16.5682	0.745126	1253.054
22-23	15.17935	0.054428	-16.6046	0.742527	1277.74
23-24	16.19945	0.04672	-16.0535	0.781894	1305.758
24-25	17.21955	0.038924	-15.8161	0.798848	1347.502
25-26	18.23965	0.038038	-19.2213	0.555624	1389.326
26-27	19.25975	0.037612	-19.0406	0.568529	1431.15
27-28	20.27985	0.040873	-13.0076	0.999461	1482.545
28-29	21.29995	0.026026	-19.9127	0.506232	1559.256
29-30	22.32005	0.033829	-19.3195	0.548605	1635.968
30-31	23.34015	0.026678	-19.6833	0.522624	1712.679
31-32	24.36025	0.027906	-20.5494	0.460756	1818.211
32-33	25.38035	0.025947	-20.2341	0.483282	1976.53

Table S2 (continued)

Depth (cm)	Corrected Depth (cm)	%C	$\delta^{13}C$ (‰)	$\%C_4$	Age (Cal. yr bp)
33-34	26.40045	0.029554	-20.7995	0.442893	2134.85
34-35	27.42055	0.031849	-18.9993	0.57148	2293.169
35-36	28.44065	0.029933	-20.4182	0.470132	2424.565
36-37	29.46075	0.025627	-16.472	0.752004	2520.557
37-38	30.48085	0.029357	-18.62	0.598573	2616.548
38-39	31.50095	0.029678	-16.559	0.745789	2712.539
39-40	32.52105	0.029328	-17.4115	0.68489	2789.565
40-41	33.54115	0.027458	-13.7114	0.949186	2848.424
41-42	34.56125	0.035299	-14.6	0.885712	2907.284
42-43	35.58135	0.029864	-16.4646	0.752531	2966.202
43-44	36.60145	0.027727	-16.9444	0.718254	3016.142
44-45	37.62155	0.026765	-14.8587	0.867237	3059.802
45-46	38.64165	0.029595	-13.2767	0.980237	3103.463
46-47	39.66175	0.026449	-14.2992	0.907203	3147.189
47-48	40.68185	0.027574	-16.0809	0.779932	3197.429
48-49	41.70195	0.026765	-12.4026	1.042669	3250.812
49-50	42.72205	0.030339	-13.7589	0.945793	3304.235
50-51	43.74215	0.026575	-15.197	0.843069	3357.689
51-52	44.76225	0.024113	-16.4019	0.757006	3383.93
52-53	45.78235	0.02142	-12.3986	1.042959	3400.965
53-54	46.80245	0.023751	-16.2711	0.766351	3418.001
54-55	47.82255	0.030079	-14.8974	0.86447	3434.954
55-56	48.84265	0.041218	-12.2747	1.051808	3447.253
56-57	49.86275	0.025802	-10.88	1.151429	3458.49
57-58	50.88285	0.038755	-12.976	1.001711	3469.711
58-59	51.90295	0.031185	-14.1544	0.91754	3481.023
59-60	52.92305	0.032001	-13.9887	0.929376	3582.343
60-61	53.94315	0.023693	-11.6205	1.098535	3693.22
61-62	54.96325	0.025252	-12.0242	1.0697	3804.105
62-63	55.98335	0.026042	-12.8227	1.012661	3914.99
63-64	57.00345	0.027819	-13.5894	0.9579	4022.262
64-65	58.02355	0.025268	-12.144	1.061146	4129.375
65-66	59.04365	0.032628	-12.7011	1.021351	4236.588
66-67	60.06375	0.031858	-13.7214	0.948473	4340.045
67-68	61.08385	0.027625	-15.0976	0.850168	4387.165
68-69	62.10395	0.023331	-13.0525	0.99625	4434.202
69-70	63.12405	0.030844	-13.912	0.934854	4481.319

Table S2 (continued)

Depth (cm)	Corrected Depth (cm)	%C	$\delta^{13}C$ (‰)	$\%C_4$	Age (Cal. yr bp)
70-71	64.14415	0.030817	-13.7048	0.949657	4533.708
71-72	65.16425	0.031429	-14.0195	0.927182	4618.666
72-73	66.18435	0.022315	-12.5899	1.029295	4703.538
73-74	67.20445	0.027374	-15.546	0.818143	4788.431
74-75	68.22455	0.02839	-15.324	0.833998	4872.26
75-76	69.24465	0.028354	-15.0866	0.850957	4952.032
76-77	70.26475	0.025635	-11.3819	1.115576	5031.803
77-78	71.28485	0.025636	-12.4993	1.035766	5111.575
78-79	72.30495	0.029931	-10.8789	1.151504	5209.797
79-80	73.32505	0.030868	-11.7423	1.089836	5351.284
80-81	74.34515	0.02553	-9.94725	1.218054	5492.772
81-82	75.36525	0.033643	-11.1504	1.132116	5634.297
82-83	76.38535	0.032439	-10.9688	1.145084	5736.234
83-84	77.40545	0.027431	-12.0865	1.065251	5772.896
84-85	78.42555	0.025557	-9.89965	1.221454	5809.62
85-86	79.44565	0.028466	-12.2914	1.050618	5846.343
86-87	80.46575	0.030527	-13.4541	0.967564	5899.322
87-88	81.48585	0.031598	-12.4736	1.037598	5971.647
88-89	82.50595	0.026994	-10.5033	1.178338	6044.022
89-90	83.52605	0.033335	-12.4229	1.041223	6116.397
90-91	84.54615	0.032779	-13.7726	0.944814	6160.377
91-92	85.56625	0.034861	-12.0264	1.069545	6179.759
92-93	86.58635	0.026072	-10.6984	1.164402	6199.199
93-94	87.60645	0.028348	-11.2267	1.126667	6218.623
94-95	88.62655	0.022872	-10.5828	1.172659	6241.764
95-96	89.64665	0.030358	-11.8884	1.079397	6267.266
96-97	90.66675	0.028686	-8.33483	1.333227	6292.769
97-98	91.68685	0.027412	-10.981	1.144214	6318.271
98-99	92.70695	0.028529	-11.9212	1.07706	6343.632
99-100	93.72705	0.028084	-11.8867	1.079523	6368.931
100-101	94.74715	0.022317	-11.3081	1.120852	6394.155
101-102	95.76725	0.026399	-12.6776	1.023026	6419.428
102-103	96.78735	0.035891	-11.7205	1.091393	6494.329
103-104	97.80745	0.040265	-10.3726	1.187672	6583.813
104-105	98.82755	0.023159	-9.94166	1.218453	6673.276
105-106	99.84765	0.023885	-11.0629	1.138364	6762.739
106-107	100.8678	0.034686	-9.6206	1.241386	6914.94

Table S2 (continued)

Depth (cm)	Corrected Depth (cm)	%C	$\delta^{13}C$ (‰)	$\%C_4$	Age (Cal. yr bp)
107-108	101.8879	0.039095	-10.4831	1.179781	7078.156
108-109	102.908	0.026665	-9.34315	1.261203	7241.463
109-110	103.9281	0.021523	-10.7091	1.163634	7404.688
110-111	104.9482	0.020644	-11.6532	1.096198	7658.168
111-112	105.9683	0.020728	-12.8962	1.007412	7918.594
112-113	106.9884	0.017886	-11.4338	1.111872	8178.927
113-114	108.0085	0.018896	-13.1098	0.992156	8437.851
114-115	109.0286	0.019356	-13.1798	0.987158	8516.501
115-116	110.0487	0.033294	-10.4769	1.180218	8595.156
117-118	112.0889	0.03293	-10.9085	1.149392	8754.025
118-119	113.109	0.025547	-11.7171	1.091639	8849.598
119-120	114.1291	0.035465	-13.0207	0.998521	8945.092
120-121	115.1492	0.032238	-10.2563	1.195975	9040.66
121-122	116.1693	0.036496	-15.1704	0.844968	9137.174
122-123	117.1894	0.04007	-9.24721	1.268057	9238.859
123-124	118.2095	0.031315	-11.9594	1.074328	9340.482
124-125	119.2296	0.020104	-10.9386	1.147242	9442.163
125-126	120.2497	0.020755	-11.8109	1.084935	9527.763
126-127	121.2698	0.019409	-12.6954	1.021759	9563.976
127-128	122.2899	0.025568	-12.2264	1.055257	9600.161
128-129	123.31	0.018522	-12.0642	1.066843	9636.303
129-130	124.3301	0.02701	-10.755	1.160358	9705.687
130-131	125.3502	0.024774	-10.7833	1.158332	9844.42
131-132	126.3703	0.0336	-8.79922	1.300056	9983.154
132-133	127.3904	0.026341	-10.2076	1.19946	10121.85
133-134	128.4105	0.026544	-9.98524	1.21534	10292.08
134-135	129.4306	0.036999	-8.9714	1.287757	10509.22
135-136	130.4507	0.030654	-9.34007	1.261423	10726.3
136-137	131.4708	0.02906	-8.80825	1.29941	10943.38
137-138	132.4909	0.027488	-9.61613	1.241705	11077.55
138-139	133.5258	0.03735	-9.92404	1.219712	11122.98
139-140	134.5846	0.030263	-11.4514	1.110616	11169.52
140-141	135.6434	0.022756	-11.1506	1.132101	11216.05
141-142	136.7022	0.029474	-11.1668	1.13094	11269.34
142-143	137.761	0.026579	-13.2098	0.985012	11326.09
143-144	138.8198	0.024014	-13.7223	0.948404	11382.84
144-145	139.8786	0.019912	-13.2852	0.979631	11439.59

Table S2 (continued)

Depth (cm)	Corrected Depth (cm)	%C	$\delta^{13}C$ (‰)	$\%C_4$	Age (Cal. yr bp)
145-146	140.9374	0.02602	-12.6854	1.022469	11525.4
146-147	141.9962	0.025836	-13.3823	0.972696	11615.08
147-148	143.055	0.019667	-15.3988	0.828657	11704.66
148-149	144.1138	0.01911	-14.8879	0.865147	11791.08
149-150	145.1726	0.024963	-13.599	0.957214	11850.5
150-151	146.2314	0.020541	-15.571	0.816359	11910
151-152	147.2902	0.019188	-16.6456	0.739601	11969.48
152-153	148.349	0.023107	-10.9743	1.14469	12061.3
153-154	149.4078	0.018707	-16.0801	0.779989	12219.06
154-155	150.4666	0.019664	-16.9531	0.717639	12376.78
155-156	151.54	0.015145	-17.327	0.690927	12536.66
160-161	156.94	0.010783	-14.3686	0.902245	12835.97
161-162	158.02	0.010243	-14.807	0.870931	12958.98
164-165	161.26	0.014405	-13.7754	0.944612	13208.29
165-166	162.34	0.020469	-12.4363	1.040266	13228.59
166-167	163.42	0.021559	-12.0534	1.067612	13248.9
167-168	164.5	0.027973	-12.3431	1.046921	13277.75
168-169	165.58	0.018426	-14.5078	0.892302	13316.46
169-170	166.66	0.017388	-15.4115	0.827751	13355.19
170-171	167.74	0.015323	-14.8902	0.864987	13393.89
172-173	169.9	0.011239	-15.0993	0.850051	13416.22
176-177	174.22	0.009677	-15.4328	0.826229	13454.13
177-178	175.3	0.00892	-15.7814	0.801329	13465.58
178-179	176.38	0.009355	-15.337	0.83307	13485.96
179-180	177.46	0.008927	-14.7749	0.873222	13522.74
180-181	178.54	0.007951	-16.5708	0.74494	13559.51
181-182	179.62	0.007458	-17.4852	0.679627	13596.28
182-183	180.7	0.007303	-17.3819	0.687006	13621.87
183-184	181.78	0.00645	-19.7296	0.519311	13641.42
184-185	182.86	0.007406	-16.2585	0.76725	13660.97
185-186	183.94	0.008462	-13.9431	0.932637	13680.42
186-187	185.02	0.007413	-17.0598	0.710017	13715.97
187-188	186.1	0.007339	-16.448	0.753714	13752.38
188-189	187.18	0.008317	-14.7398	0.87573	13788.87
189-190	188.26	0.008558	-14.9138	0.863298	13825.73
190-191	189.34	0.007441	-17.1435	0.704033	13864.07
191-192	190.42	0.009667	-12.6516	1.024883	13902.45

Table S2 (continued)

Depth (cm)	Corrected Depth (cm)	%C	$\delta^{13}C$ (‰)	$\%C_4$	Age (Cal. yr bp)
192-193	191.5	0.005925	-17.431	0.683497	13940.85
193-194	192.58	0.009158	-12.2884	1.050828	14005.06
194-195	193.66	0.007417	-14.1004	0.921403	14091.57
195-196	194.74	0.013555	-9.94068	1.218523	14178.07
196-197	195.82	0.009874	-10.7106	1.16353	14264.58
200-201	200.14	0.011555	-10.2034	1.199759	14392.37
204-205	204.5	0.024539	-10.133	1.204789	14567.95
205-206	205.5	0.01975	-8.71999	1.305715	14634.05
206-207	206.5	0.017455	-14.3439	0.904006	14700.15
207-208	207.5	0.016673	-8.27072	1.337806	14766.25
208-209	208.5	0.015195	-8.29802	1.335855	14846.7
210-211	210.5	0.024718	-11.7586	1.088673	15036.3
211-212	211.5	0.03254	-8.18618	1.343845	15131.1
213-214	213.5	0.02528	-11.269	1.123641	15250.8
219-220	219.5	0.022959	-6.86601	1.438142	15452.85
220-221	220.5	0.030662	-10.1069	1.206651	15475.25
221-222	221.5	0.028643	-10.5786	1.172958	15496.75
237-238	237.5	0.0224	-8.0859	1.351007	16769.75
238-239	238.5	0.019887	-10.1847	1.201092	16876.4
239-240	239.5	0.020863	-7.8711	1.36635	16983.05
240-241	240.5	0.033068	-8.23339	1.340472	17057.1
244-245	244.5	0.036261	-8.08832	1.350834	17281.5
245-246	245.5	0.04999	-8.03357	1.354745	17440.3
247-248	247.5	0.028846	-8.92846	1.290824	17758
248-249	248.5	0.042692	-8.17556	1.344603	17846.95
249-250	249.5	0.032174	-10.0026	1.214096	17866.05
250-251	250.5	0.029406	-9.35834	1.260119	17885.2
252-253	252.5	0.028546	-8.59655	1.314532	17948.95
253-254	253.5	0.033283	-9.23393	1.269005	18019.05
256-257	256.5	0.03796	-10.2909	1.193506	18201.15
258-259	258.5	0.027822	-9.74978	1.232159	18228.2
260-261	260.5	0.033209	-10.3357	1.19031	18278.85
261-262	261.5	0.028841	-10.1716	1.202031	18339.55
262-263	262.5	0.030653	-10.382	1.187003	18400.25
263-264	263.5	0.031785	-10.207	1.199502	18460.95
264-265	264.5	0.025204	-9.80388	1.228294	18501.95
267-268	267.5	0.026748	-7.91248	1.363394	18565.75

Table S2 (continued)

Depth (cm)	Corrected Depth (cm)	%C	$\delta^{13}C$ (‰)	$\%C_4$	Age (Cal. yr bp)
268-269	268.5	0.029326	-10.2238	1.198299	18592.45
269-270	269.5	0.035657	-11.0135	1.141891	18624.5
272-273	272.5	0.047111	-9.1511	1.274921	18715.65
274-275	274.5	0.032068	-10.0791	1.208638	18759.95
275-276	275.5	0.029886	-11.2406	1.125673	18782.05
279-280	279.5	0.028464	-9.83171	1.226306	18816.05
284-285	284.5	0.029991	-8.64668	1.310952	19075.35
285-286	285.5	0.028113	-10.2737	1.194734	19100.25

Table S3: Radiocarbon dates as published by Cooke et al. (2003).

Depth (cm)	Material	RC (yBP)	stddev
15-20	gelatin	1500	60
25-30	gelatin	2330	60
51	charcoal	3190	70
60-65	gelatin	4000	60
90-95	gelatin	5320	60
76-78	humins	5400	70
105-110	gelatin	7700	80
120-125	gelatin	8630	60
145-150	gelatin	10310	70
155-160	liquefied gelatin	11310	60
165-170	gelatin	11410	70
185-190	gelatin	11550	70
195-200	gelatin	12110	90
220-225	gelatin	12570	80
270-275	gelatin	13940	100
210-215	liquefied gelatin	14400	80
235-240	gelatin	14700	90
260	humic acid	15290	90
295-300	gelatin	16240	100
315-320	gelatin	16510	100
338-343	humic acid	16610	110
300-305	gelatin	16620	110
345-350	gelatin	16770	100

Table S4: Age-depth model. 95% probability intervals are in calendar years BP.

Depth (cm)	Average Age (Cal. yr BP)	Lower 95%	Upper 95%	Depth (cm)	Average Age (Cal. yr BP)	Lower 95%	Upper 95%
0	-43	-691	484	35	2932.6	2353	3033
1	16.3	-505	490	36	2990.4	2386	3106
2	75.6	-323	542	37	3033.2	2442	3142
3	134.9	-152	598	38	3076	2452	3227
4	194.1	-25	635	39	3118.8	2508	3278
5	325.2	18	673	40	3161.7	2544	3319
6	456.2	45	800	41	3214.1	2596	3336
7	587.2	82	962	42	3266.4	2671	3401
8	718.3	114	1089	43	3318.8	2718	3448
9	838.9	260	1090	44	3371.2	2745	3495
10	959.5	374	1154	45	3387.9	2821	3506
11	1080.1	415	1225	46	3404.6	2870	3550
12	1200.7	481	1376	47	3421.3	2948	3588
13	1225	641	1386	48	3437.9	2936	3646
14	1249.2	784	1429	49	3449	3091	3706
15	1273.4	851	1456	50	3460	3175	3710
16	1297.6	955	1580	51	3471	3266	3736
17	1338.5	1148	1593	52	3482.1	3313	3878
18	1379.5	1308	1638	53	3590.7	3409	3924
19	1420.5	1350	1770	54	3699.4	3472	4057
20	1461.5	1366	1966	55	3808.1	3491	4226
21	1536.7	1448	2048	56	3916.8	3523	4353
22	1611.9	1495	2135	57	4021.9	3612	4387
23	1687.1	1550	2225	58	4126.9	3675	4450
24	1762.3	1580	2340	59	4232	3725	4510
25	1917.5	1758	2358	60	4337.1	3780	4615
26	2072.7	1905	2395	61	4383.3	3954	4699
27	2227.9	2012	2492	62	4429.4	4154	4784
28	2383.1	2064	2564	63	4475.6	4288	4853
29	2477.2	2139	2679	64	4521.7	4351	4951
30	2571.3	2179	2724	65	4605	4433	5073
31	2665.4	2214	2789	66	4688.2	4449	5254
32	2759.5	2223	2893	67	4771.4	4505	5445
33	2817.2	2277	2922	68	4854.7	4515	5675
34	2874.9	2305	3030	69	4932.9	4604	5729

Table S4 (continued)

Depth (cm)	Average Age (Cal. yr BP)	Lower 95%	Upper 95%	Depth (cm)	Average Age (Cal. yr BP)	Lower 95%	Upper 95%
70	5011.1	4693	5763	107	8181.9	8043	8623
71	5089.3	4741	5866	108	8437.2	8202	8722
72	5167.5	4796	6026	109	8514.3	8314	8799
73	5306.2	4874	6094	110	8591.4	8403	8933
74	5444.9	4898	6158	111	8668.6	8481	9091
75	5583.6	4921	6226	112	8745.7	8520	9290
76	5722.4	4965	6310	113	8839.4	8592	9337
77	5758.3	5005	6355	114	8933	8634	9394
78	5794.3	5070	6405	115	9026.7	8666	9521
79	5830.3	5180	6490	116	9120.3	8693	9618
80	5866.3	5230	6575	117	9220	8803	9648
81	5937.2	5279	6644	118	9319.6	8923	9698
82	6008.1	5314	6709	119	9419.3	8951	9796
83	6079.1	5359	6759	120	9518.9	8971	9936
84	6150	5409	6829	121	9554.4	9190	9940
85	6169	5457	6872	122	9589.9	9339	9974
86	6188	5521	6921	123	9625.3	9477	9997
87	6207.1	5640	7030	124	9660.8	9539	10229
88	6226.1	5710	7055	125	9796.8	9619	10299
89	6251.1	5812	7092	126	9932.8	9645	10370
90	6276.1	5869	7124	127	10068.8	9680	10465
91	6301.1	5898	7183	128	10204.7	9700	10675
92	6326.1	5920	7260	129	10417.6	9789	10754
93	6350.9	6039	7294	130	10630.4	9838	10878
94	6375.7	6105	7335	131	10843.2	9882	10982
95	6400.4	6167	7437	132	11056	9916	11196
96	6425.2	6175	7545	133	11099.9	10035	11245
97	6513	6315	7730	134	11143.8	10115	11360
98	6600.7	6393	7813	135	11187.8	10195	11425
99	6688.4	6476	7911	136	11231.7	10230	11575
100	6776.1	6512	8117	137	11285.3	10422	11632
101	6936.1	6744	8184	138	11338.9	10481	11721
102	7096.1	6882	8282	139	11392.5	10661	11841
103	7256.2	7091	8456	140	11446.1	10736	11976
104	7416.2	7219	8559	141	11530.7	10834	12004
105	7671.4	7492	8552	142	11615.4	10959	12029
106	7926.7	7756	8586	143	11700	11069	12174

Table S4 (continued)

Depth (cm)	Average Age (Cal. yr BP)	Lower 95%	Upper 95%	Depth (cm)	Average Age (Cal. yr BP)	Lower 95%	Upper 95%
144	11784.7	11027	12262	181	13627.3	13345	13980
145	11840.8	11328	12283	182	13645.4	13328	13963
146	11897	11482	12357	183	13663.5	13392	13997
147	11953.2	11647	12422	184	13681.5	13410	14035
148	12009.3	11682	12517	185	13715.3	13438	14078
149	12158.3	11864	12549	186	13749	13445	14090
150	12307.3	11957	12622	187	13782.8	13474	14104
151	12456.2	12007	12752	188	13816.5	13480	14130
152	12605.2	12033	12868	189	13852	13500	14275
153	12636.1	12173	12903	190	13887.5	13520	14195
154	12667	12298	12973	191	13923.1	13556	14426
155	12698	12388	13053	192	13958.6	13569	14374
156	12728.9	12453	13188	193	14038.7	13635	14465
157	12842.8	12544	13214	194	14118.8	13695	14525
158	12956.7	12667	13257	195	14198.9	13726	14681
159	13070.6	12744	13294	196	14279	13771	14746
160	13184.5	12797	13337	197	14306	13833	14823
161	13203.4	12846	13361	198	14333.1	13896	14876
162	13222.2	12870	13380	199	14360.1	13940	14930
163	13241	12889	13404	200	14387.2	13938	14973
164	13259.8	12908	13448	201	14424.1	14031	15086
165	13295.7	12964	13449	202	14461	14068	15073
166	13331.5	13006	13476	203	14498	14121	15196
167	13367.4	13032	13502	204	14534.9	14158	15258
168	13403.2	13053	13533	205	14601	14236	15321
169	13410.1	13073	13548	206	14667.1	14263	15353
170	13416.9	13085	13570	207	14733.2	14310	15430
171	13423.8	13119	13619	208	14799.3	14347	15507
172	13430.6	13154	13679	209	14894.1	14433	15563
173	13441.2	13193	13703	210	14988.9	14439	15629
174	13451.8	13203	13723	211	15083.7	14475	15725
175	13462.4	13220	13815	212	15178.5	14642	15947
176	13473	13195	13810	213	15226.7	14689	15984
177	13507.1	13252	13827	214	15274.9	14773	16048
178	13541.1	13274	13854	215	15323	14836	16141
179	13575.2	13281	13871	216	15371.2	14909	16254
180	13609.2	13322	13907	217	15394.5	14957	16267

Table S4 (continued)

Depth (cm)	Average Age (Cal. yr BP)	Lower 95%	Upper 95%	Depth (cm)	Average Age (Cal. yr BP)	Lower 95%	Upper 95%
218	15417.9	14964	16359	255	18124.2	16716	18406
219	15441.2	14996	16396	256	18194.4	16813	18463
220	15464.5	15013	16423	257	18207.9	16879	18489
221	15486	15034	16479	258	18221.4	16806	18486
222	15507.5	15064	16529	259	18235	16872	18502
223	15529	15057	16587	260	18248.5	16904	18529
224	15550.5	15130	16695	261	18309.2	16983	18543
225	15655.9	15173	16743	262	18369.9	17091	18561
226	15761.4	15160	16840	263	18430.6	16980	18590
227	15866.9	15244	16929	264	18491.3	17104	18649
228	15972.3	15272	17117	265	18512.6	17160	18690
229	15998.7	15478	17148	266	18533.8	17081	18691
230	16025.1	15631	17166	267	18555.1	17112	18727
231	16051.5	15695	17220	268	18576.4	17262	18747
232	16077.9	15724	17344	269	18608.5	17402	18767
233	16210.8	15776	17451	270	18640.5	17413	18808
234	16343.8	15839	17429	271	18672.6	17303	18833
235	16476.8	15897	17522	272	18704.6	17393	18988
236	16609.8	15950	17665	273	18726.7	17503	18883
237	16716.4	15855	17715	274	18748.9	17479	18909
238	16823.1	16009	17819	275	18771	17539	18924
239	16929.7	15987	17877	276	18793.1	17585	19050
240	17036.4	16125	17920	277	18799.7	17657	18982
241	17077.8	16094	17944	278	18806.2	17801	19036
242	17119.2	16060	17980	279	18812.8	17699	19109
243	17160.6	16160	18005	280	18819.3	17883	19193
244	17202.1	16186	18096	281	18880.2	18053	19223
245	17360.9	16307	18097	282	18941.1	18097	19232
246	17519.7	16352	18247	283	19002	18111	19291
247	17678.6	16406	18161	284	19062.9	18169	19339
248	17837.4	16499	18189	285	19087.8	18206	19366
249	17856.5	16474	18194	286	19112.7	18281	19406
250	17875.6	16510	18235	287	19137.6	18287	19427
251	17894.8	16552	18252	288	19162.5	18327	19462
252	17913.9	16598	18323	289	19217	18378	19488
253	17984	16638	18378	290	19271.4	18468	19523
254	18054.1	16638	18383	291	19325.9	18523	19558

Table S4 (continued)

Depth (cm)	Average Age (Cal. yr BP)	Lower 95%	Upper 95%
292	19380.4	18568	19593
293	19417.1	18671	19611
294	19453.8	18764	19634
295	19490.5	18868	19668
296	19527.2	18912	19707
297	19556.7	18961	19721
298	19586.2	19007	19727
299	19615.7	19038	19748
300	19645.1	19061	19776
301	19663.3	19124	19799
302	19681.4	19140	19835
303	19699.6	19156	19881
304	19717.7	19187	19932
305	19724.5	19204	19964
306	19731.3	19215	19985
307	19738.1	19244	20014
308	19744.8	19279	20069
309	19756.2	19300	20100
310	19767.5	19319	20134
311	19778.8	19386	20176
312	19790.1	19397	20202
313	19791.7	19432	20222
314	19793.3	19431	20261
315	19794.8	19496	20291
316	19796.4	19510	20315
317	19817.5	19556	20336
318	19838.6	19591	20361
319	19859.7	19610	20380
320	19880.9	19642	20422
321	19907.2	19663	20438
322	19933.5	19693	20493
323	19959.8	19694	20514
324	19986.1	19715	20560
325	19993.1	19731	20586
326	20000	19762	20622
327	20006.9	19763	20653
328	20013.8	19804	20729
329	20028.4	19828	20763
330	20043	19827	20827
331	20057.5	19831	20811
332	20072.1	19855	20865
333	20093.4	19895	20900
334	20114.6	19910	20950
335	20135.9	19923	20973
336	20157.1	19931	21016
337	20183.6	19955	21045
338	20210.1	19966	21116
339	20236.6	19977	21142
340	20263.1	19987	21182
341	20275.8	20031	21206
342	20288.6	20048	21308
343	20301.3	20064	21349
344	20314	20084	21364
345	20330.5	20098	21398
346	20347	20161	21426
347	20363.4	20176	21456
348	20379.9	20184	21494

APPENDIX B: MATLAB MODELING SCRIPTS

Script 1: Distribution change with relative season length

```
% Distribution change with relative season length
clear;
clc;
%%

%=====================================
% Inputs
%=====================================

my_mean = -7.2;       % Resting position of annual cycle (in permil)
c13_std = 1.59;       % Std. deviation for each point (in permil)
amplitude = 0;        % Amplitude (as a percentage of 7 permil)
C3_season1 = 20;      % Starting C3 season length (as % of year)
C3_season2 = 80;      % Ending C3 season length (as % of year)

%%

%=====================================
% Manufacturing Synthetic Time Series'
%=====================================
nyear = 1000;                 % Length of time series (# of years)
len = nyear*100;              % Year broken into 100 blocks (total # of teeth)

me = zeros(C3_season2-C3_season1+1,1);   % Creation of median vector
sd = zeros(C3_season2-C3_season1+1,1);   % Creation of std. dev. vector
sk = zeros(C3_season2-C3_season1+1,1);   % Creation of skewness vector

for season=C3_season1:C3_season2

   season

   std_year = zeros(100,1);

   for s=1:season
      std_year(s) = -amplitude/100*7*sin(pi/(100*(season)/100)*s)+my_mean;
                                % C3 season sine wave creation
   end
```

```
   for w=season+1:100
      std_year(w) = amplitude/100*7*sin(pi/(100*(100-season)/100)*(w-
season))+my_mean;              % C4 season sine wave creation
   end

   basin=zeros(100,nyear);
   prts=zeros(len,1);

   for i=1:nyear
      basin(:,i)=std_year;                    % Populate the number of years
   end

   std_years = reshape(basin,len,1);          % Change to vector

   for c=1:len
      prts(c) = std_years(c) + c13_std*randn;
                        % Sample years and apply individual variation
   end

   sd(season-C3_season1+1) = std(prts);       % Calculate standard deviation of samples
   sk(season-C3_season1+1) = skewness(prts);        % Calculate skewness of samples
   me(season-C3_season1+1) = median(prts);          % Calculate median of samples

   if season==99
      figure(4)                            % Histogram for 99% C3 season
      clf;
      hold on;
      hist(prts,30);
      h = findobj(gca,'Type','patch');
      set(h,'FaceColor','k','EdgeColor','w');
   end

   if season==75
      figure(5)                            % Histogram for 75% C3 season
      clf;
      hold on;
      hist(prts,30);
      h = findobj(gca,'Type','patch');
      set(h,'FaceColor','k','EdgeColor','w');
   end

end
%%
```

```
%=====================================
% Data Export
%=====================================

figure(1)                       % Create figure of standard deviation vs. C3 season length
clf;
hold on;
plot(1:length(sd),sd,'k');
set(gca,'FontName','Myriad Pro','fontsize',13,'FontWeight','bold');
set(gca,'XGrid','on');
title('Standard Deviation');
xlabel('% C3 Season');
ylabel('\delta^{13}C');

figure(2)                       % Create figure of skewness vs. C3 season length
clf;
hold on;
plot(1:length(sk),sk,'k');
set(gca,'FontName','Myriad Pro','fontsize',13,'FontWeight','bold');
set(gca,'XGrid','on');
title('Skewness');
xlabel('% C3 Season');
ylabel('Skewness');

figure(3)                       % Create figure of median vs. C3 season length
clf;
hold on;
plot(1:length(me),me,'k');
set(gca,'FontName','Myriad Pro','fontsize',13,'FontWeight','bold');
set(gca,'XGrid','on');
title('Median');
xlabel('% C3 Season');
ylabel('\delta^{13}C');

fid_sd=fopen('l_sd.txt','w');           % Create text file for standard deviations
for i=1:length(sd)
   fprintf(fid_sd,'%0.15f\r\n',sd(i));
end
fclose(fid_sd);

fid_sk=fopen('l_skew.txt','w');         % Create text file for skewness
for i=1:length(sk)
   fprintf(fid_sk,'%0.15f\r\n',sk(i));
```

```
end
fclose(fid_sk);

fid_me=fopen('l_medi.txt','w');          % Create text file for median
for i=1:length(me)
   fprintf(fid_me,'%0.15f\r\n',me(i));
end
fclose(fid_me);
```

Script 2: Distribution change with amplitude

```
% Distribution change with amplitude
clear;
clc;
%%

%=====================================
% Inputs
%=====================================

my_mean = -7.2;       % Resting position of annual cycle (in permil)
c13_std = 1.59;       % Std. deviation for each point (in permil)
C3_season = 50;       % Length of C3 season (as % of year)
Amplitude1 = 0;       % Beginning amplitude (as % of 7 permil)
Amplitude2 = 100;     % Ending amplitude (as % of 7 permil)

%%

%=====================================
% Manufacturing Synthetic Time Series
%=====================================

nyear = 1000;         % Length of time series (# of years)
len = nyear*100;      % Year broken into 100 blocks (total # of teeth)

sd = zeros(Amplitude2-Amplitude1+1,1);    % Creation of stdev vector
sk = zeros(Amplitude2-Amplitude1+1,1);    % Creation of skewness vector
me = zeros(Amplitude2-Amplitude1+1,1);    % Creation of median vector

for amp=Amplitude1:Amplitude2

   amp

   std_year = zeros(100,1);

   for s=1:C3_season
      std_year(s) = -amp/100*7*sin(pi/(100*(C3_season)/100)*s)+my_mean;
                  % C3 season sine wave creation
   end

   for w=C3_season+1:100
      std_year(w) = amp/100*7*sin(pi/(100*(100-C3_season)/100)*(w-
```

```
C3_season))+my_mean;
                % C4 season sine wave creation
   end

   basin=zeros(100,nyear);
   prts=zeros(len,1);

   for i=1:nyear
      basin(:,i)=std_year;          % Populate the number of years
   end

   std_years = reshape(basin,len,1);

   for c=1:len
      prts(c) = std_years(c) + c13_std*randn;
                % Sample from years and apply individual variation
   end

   sd(amp-Amplitude1+1) = std(prts);                % Calculate stdev
   sk(amp-Amplitude1+1) = skewness(prts);           % Calculate skewness
   me(amp-Amplitude1+1) = median(prts);             % Calculate median

   if amp==50
      figure(4)         % Histogram of 50% amplitude
      clf;
      hold on;
      hist(prts,30);
      h = findobj(gca,'Type','patch');
      set(h,'FaceColor','k','EdgeColor','w');
   end

   if amp==100
      figure(5)         % Histogram of 100% amplitude
      clf;
      hold on;
      hist(prts,30);
      h = findobj(gca,'Type','patch');
      set(h,'FaceColor','k','EdgeColor','w');
   end

end
```

```
%%

%=====================================
% Data Export
%=====================================

figure(1)                       % Figure of stdev against amplitude
clf;
hold on;
plot(1:length(sd),sd,'k');
set(gca,'FontName','Myriad Pro','fontsize',13,'FontWeight','bold');
set(gca,'XGrid','on');
title('Standard Deviation');
xlabel('%C3 winter - summer');
ylabel('\delta^{13}C');

figure(2)                       % Figure of skewness against amplitude
clf;
hold on;
plot(1:length(sk),sk,'k');
set(gca,'FontName','Myriad Pro','fontsize',13,'FontWeight','bold');
set(gca,'XGrid','on');
title('Skewness');
xlabel('%C3 winter - summer');
ylabel('Skewness');

figure(3)                       % Figure of median against amplitude
clf;
hold on;
plot(1:length(me),me,'k');
set(gca,'FontName','Myriad Pro','fontsize',13,'FontWeight','bold');
set(gca,'XGrid','on');
title('Median');
xlabel('%C3 winter - summer');
ylabel('\delta^{13}C');

fid_sd=fopen('s_sd.txt','w');          % Create text file for stdev
for i=1:length(sd)
   fprintf(fid_sd,'%0.15f\r\n',sd(i));
end
fclose(fid_sd);
```

```
fid_sk=fopen('s_sk.txt','w');          % Create text file for skewness
for i=1:length(sk)
   fprintf(fid_sk,'%0.15f\r\n',sk(i));
end
fclose(fid_sk);

fid_me=fopen('s_me.txt','w');          % Create text file for median
for i=1:length(me)
   fprintf(fid_me,'%0.15f\r\n',me(i));
end
fclose(fid_me);
```

Script 3: Precision change with sample size

```
% Sample size and precision
clear;
clc;
%%

%====================================
% Input
%====================================

my_mean = -7.2;       % Resting position of annual cycle (in permil)
c13_std = 1.59;       % Std. deviation of individual points (in permil)
amplitude = 16;       % Amplitude (as % of 7)
C3_season = 20;       % C3 Season length (as % of year)
tooth1 = 3;           % Minimum number of teeth (needs to be at least 3)
tooth2 = 100;         % Maximum number of teeth

%%

%====================================
% Manufacturing Synthetic Time Series
%====================================

nyear = 1000;                 % Number of years
len = nyear*100;              % Number of total teeth in population

std_year1 = zeros(100,1);

for w=1:C3_season
   std_year1(w) = -amplitude/100*7*sin(pi/(100*(C3_season)/100)*w)+my_mean;
          % C3 season sine wave creation
end

for s=C3_season+1:100
   std_year1(s) = amplitude/100*7*sin(pi/(100*(100-C3_season)/100)*(s-
C3_season))+my_mean;
          % C4 season sine wave creation
end

basin1=zeros(100,nyear);
prts1=zeros(len,1);
```

```
for p=1:nyear
   basin1(:,p)=std_year1;          % Populate the number of years
end

std_years1 = reshape(basin1,len,1);

for i=1:len
   prts1(i) = std_years1(i) + c13_std*randn;
            % Create population and apply individual variation
end

nor_sd = std(prts1);              % Population Std. Dev.
nor_sk = skewness(prts1);     % Population Skewness
nor_med = median(prts1);      % Population median

figure(1)                 % Time series
clf;
plot(1:len,prts1,'k');
set(gca,'FontName','Myriad Pro','fontsize',13,'FontWeight','bold')
set(gca,'XGrid','on')
title('Normal Time Series');
xlabel('Month');
ylabel('\delta^{13}C');

%%

%=====================================
% Monte Carlo Simulations
%=====================================

sd_sd1 = zeros(tooth2-tooth1+1,1);   % Error of stdev for each sample size
sk_sd1 = zeros(tooth2-tooth1+1,1);   % Error of skew for each sample size
me_sd1 = zeros(tooth2-tooth1+1,1);  % Error of median for each sample size

for  tooth_spread = tooth1:tooth2

num = tooth_spread;             % Number of land forams aka teeth
run = 10000;                    % Number of MCs
anerr = 0.02;                   % Analytical error (for d13C)

mcstd1 = zeros(run,1);          % Stdev for each run
mcskew1 = zeros(run,1);         % Skewness for each run
mcmed1 = zeros(run,1);          % Median for each run
```

```
   for mc = 1:run                % Monte Carlo Loop
      mcp1 = zeros(num,1);    % Monte Carlo Pick
      for j=1:num                % Picking Loop
         k = ceil((len)*rand);
         mcp1(j) = prts1(k) + anerr*randn;
               % Tooth selection and analytical error application
      end
      mcstd1(mc) = std(mcp1);                % Calculate stdev for run
      mcskew1(mc) = skewness(mcp1);       % Calculate skewness for run
      mcmed1(mc) = median(mcp1);           % Calculate median for run
   end

%=====================================
% Data Analysis
%=====================================

%---- Time Series ----

mc_sd_sd1 = std(mcstd1);              % Calculating stdev error
mc_sk_sd1 = std(mcskew1);           % Calculating skewness error
mc_me_sd1 = std(mcmed1);           % Calculating median error

sd_sd1(tooth_spread-tooth1+1) = mc_sd_sd1;
sk_sd1(tooth_spread-tooth1+1) = mc_sk_sd1;
me_sd1(tooth_spread-tooth1+1) = mc_me_sd1;

tooth_spread

end

%% True population value display
format short;
disp('Teeth!!!');disp(' ');
disp('Time Series');
disp(['True SD: ',num2str(nor_sd),'‰']);
disp(['True Skewness: ',num2str(nor_sk)]);
disp(['True Median: ',num2str(nor_med)]);

%%

figure(2)      % Histogram of population
clf;
hold on;
```

```
hist(prts1,30);
h = findobj(gca,'Type','patch');
set(h,'FaceColor','k','EdgeColor','w');

figure(3)       % Stdev of stdev vs. sample size
clf;
hold on;
plot(1:tooth2-tooth1+1,sd_sd1,'k');
set(gca,'FontName','Myriad Pro','fontsize',13,'FontWeight','bold');
set(gca,'XGrid','on');
title('Standard Deviation of Standard Deviation (Series 1)');
xlabel('# of Teeth');
ylabel('\delta^{13}C');

figure(4)       % Stdev of skewness vs. sample size
clf;
hold on;
plot(1:tooth2-tooth1+1,sk_sd1,'k');
set(gca,'FontName','Myriad Pro','fontsize',13,'FontWeight','bold');
set(gca,'XGrid','on');
title('Standard Deviation of Skewness (Series 1)');
xlabel('# of Teeth');
ylabel('Skewness');

figure(5)       % Stdev of median vs. sample size
clf;
hold on;
plot(1:tooth2-tooth1+1,me_sd1,'k');
set(gca,'FontName','Myriad Pro','fontsize',13,'FontWeight','bold');
set(gca,'XGrid','on');
title('Standard Deviation of Median (Series 1)');
xlabel('# of Teeth');
ylabel('Median');

fid1 = fopen('sd1.txt','w');    % Create stdev of stdev text file
for i=1:length(sd_sd1)
   fprintf(fid1,'%0.15f\r\n',sd_sd1(i));
end
fclose(fid1);

fid2 = fopen('skew1.txt','w');  % Create stdev of skewness text file
for i=1:length(sk_sd1)
   fprintf(fid2,'%0.15f\r\n',sk_sd1(i));
```

```
end
fclose(fid2);

fid3 = fopen('medi1.txt','w');   % Create stdev of median text file
for i=1:length(me_sd1)
    fprintf(fid3,'%0.15f\r\n',me_sd1(i));
end
fclose(fid3);
```

References

Abul-Fatih, H. A., and F. A. Bazzaz. 1979. The biology of *Ambrosia trifida* L. II germination, emergence, growth, and survival. *New Phytologist* 83:817–827.

Angevine, M. W., and B. F. Chabot. 1979. Seed germination syndromes in higher plants. In: Solbrig, O. T., Jain, S., Johnson, G. B., Raven, P. H. (eds) *Topics in Plant Population Biology*. Columbia University Press, New York.

Arguez, A., S. Applequist, R. Vose, I. Durre, M. Squires, and X. Yin. 2012. NOAA's 1981-2010 climate normals methodology of temperature-related normals. *NCDC Report.* 7 pp.

Asmerom, Y., V. J. Polyak, and S. J. Burns. 2010. Variable winter moisture in the southwestern United States linked to rapid glacial climate shifts. *Nature Geoscience* 3:114–117.

Balesdent, J., C. Girardin, and A. Mariotti. 1993. Site-related $\delta^{13}C$ of tree leaves and soil organic matter in a temperate forest. *Ecology* 74:1713–1721.

Bedaso, Z. K., J. G. Wynn, Z. Alemseged, and D. Geraads. 2013. Dietary and paleoenvironmental reconstruction using stable isotopes of herbivore tooth enamel from middle Pliocene Dikika, Ethiopia: implication for *Australopithecus afarensis* habitat and food resources. *Journal of Human Evolution* 64:21–38.

Berger, A. L. 1978. Long-term variations of daily insolation and quaternary climatic changes. *Journal of the Atmospheric Sciences* 35:2362–2367.

Besnard, G., A. M. Muasya, F. Russier, E. H. Roalson, N. Salamin, and P.-A. Christin. 2009. Phylogenomics of C_4 photosynthesis in sedges (Cyperaceae): multiple appearances and genetic convergence. *Molecular Biology and Evolution* 26:1909–1919.

Blaauw, M., and J. A. Christen. 2011. Flexible paleoclimate age-depth models using an autoregressive gamma process. *Bayesian Analysis* 6:457–474.

Bomar, G. W. 1995. *Texas Weather: Second Edition, Revised*. University of Texas Press. Austin, TX. 287 pp.

Bond, W. J. 2008. What limits trees in C_4 grasslands and savannas? *Annual Review of Ecology, Evolution, and Systematics* 39:641–659.

Boutton, T. W., S. R. Archer, A. J. Midwood, S. F. Zitzer, and R. Bol. 1998. $\delta^{13}C$ values of soil organic carbon and their use in documenting vegetation change in a subtropical savanna ecosystem. *Geoderma* 82:5–41.

Brewer, N. R. 2006. Biology of the rabbit. *Journal of the American Association for Laboratory Animal Science* 45:8–24.

Cerling, T. E. 1984. The stable isotopic composition of modern soil carbonate and its relationship to climate. *Earth and Planetary Science Letters* 71:229–240.

Cerling, T. E., and Z. D. Sharp. 1996. Stable carbon and oxygen isotope analysis of fossil tooth enamel using laser ablation. *Palaeogeography, Palaeoclimatology, Palaeoecology* 126:173–186.

Cerling, T. E., J. M. Harris, B. J. Macfadden, M. G. Leakey, J. Quadek, V. Eisenmann, and J. R. Ehleringer. 1997. Global vegetation change through the Miocene/Pliocene boundary. *Nature* 389:153–158.

Cerling, T. E., and J. M. Harris. 1999. Carbon isotope fractionation between diet and bioapatite in ungulate mammals and implications for ecological and paleoecological studies. *Oecologia* 120:347–363.

Chapman, J. A., and G. R. Willner. 1978. *Sylvilagus audubonii. Mammalian Species* 106:1–4.

Christin, P.-A., G. Besnard, E. Samaritani, M. R. Duvall, T. R. Hodkinson, V. Savolainen, and N. Salamin. 2008. Oligocene CO_2 decline promoted C_4 photosynthesis in grasses. *Current Biology* 18:37–43.

Cooke, M. J., L. A. Stern, J. L. Banner, L. E. Mack, T. W. J. Stafford, and R. S. I. Toomey. 2003. Precise timing and rate of massive late Quaternary soil denudation. *Geology* 31:853–856.

Correll, D. S., and M. C. Johnston 1970. *Manual of the Vascular Plants of Texas*. Texas Research Foundation. Renner, TX. 1881 pp.

Dalke, P. D., and P. R. Sime. 1941. Food habits of the eastern and New England cottontails. *The Journal of Wildlife Management* 5:216–228.

Deniro, M. J., and S. Epstein. 1978. Influence of diet on the distribution of carbon isotopes in animals. *Geochimica et Cosmochimica Acta* 42:495–506.

DiMiceli, C. M., M. L. Carroll, R. A. Sohlberg, C. Huang, M. C. Hansen, and J. R. G. Townshend. 2011. Annual Global Automated MODIS Vegetation Continuous Fields (MOD44B) at 250 m Spatial Resolution for Data Years Beginning Day 65, 2000 - 2010, Collection 5. University of Maryland, College Park, MD. http://www.landcover.org/data/vcf/

Durre, I., M. F. Squires, R. S. Vose, A. Arguez, S. Applequist, and X. Yin. 2011. Computational procedures for the 1981-2010 normals: precipitation, snowfall, and snow depth. *NCDC Report.* 11 pp.

Ehleringer, J. R., C. B. Field, Z. Lin, and C. Kuo. 1986. Leaf carbon isotope and mineral composition in subtropical plants along an irradiance cline. *Oecologia* 70:520–526.

Ehleringer, J. R. 1993. Variation in leaf carbon isotope discrimination in *Encelia farinosa*: implications for growth, competition, and drought survival. *Oecologia* 95:340–346.

Ehleringer, J. R., T. E. Cerling, and B. R. Helliker. 1997. C_4 photosynthesis, atmospheric CO_2, and climate. *Oecologia* 112:285–299.

Feldhamer, G. A., B. C. Thompson, and J. A. Chapman, eds. 2003. *Wild Mammals of North America: Biology, Management, and Conservation*. The Johns Hopkins University Press. Baltimore, MD. 1216 pp.

Feranec, R. S., E. A. Hadly, and A. Paytan. 2009. Stable isotopes reveal seasonal competition for resources between late Pleistocene bison (Bison) and horse (Equus) from Rancho La Brea, southern California. *Palaeogeography, Palaeoclimatology, Palaeoecology* 271:153–160.

Feranec, R. S., E. A. Hadly, and A. Paytan. 2010. Isotopes reveal limited effects of middle Pleistocene climate change on the ecology of mid-sized mammals. *Quaternary International* 217:43–52.

Forbes, M. S., M. J. Kohn, E. A. Bestland, and R. T. Wells. 2010. Late Pleistocene environmental change interpreted from $\delta^{13}C$ and $\delta^{18}O$ of tooth enamel from the Black Creek Swamp Megafauna site, Kangaroo Island, South Australia. *Palaeogeography, Palaeoclimatology, Palaeoecology* 291:319–327.

Fowler, N. L., and D. W. Dunlap. 1986. Grassland vegetation of the eastern Edwards Plateau. *American Midland Naturalist* 115:146–155.

Friedli, H., H. Lötscher, H. Oeschger, U. Siegenthaler, and B. Stauffer. 1986. Leaf carbon isotope and mineral composition in subtropical plants along an irradiance cline. *Nature* 324:237–238.

Hibbard, C. W. 1949. Techniques of collecting microvertebrate fossils. *Contributions from the Museum of Paleontology, University of Michigan* 8:7-19

Hobson, K., and J. Sease. 1998. Stable isotope analyses of tooth annuli reveal temporal dietary records : An Example Using Stellar Sea Lions. *Marine Mammal Science* 14:116–129.

Hoppe, K. A, S. M. Stover, J. R. Pascoe, and R. Amundson. 2004. Tooth enamel biomineralization in extant horses: implications for isotopic microsampling. *Palaeogeography, Palaeoclimatology, Palaeoecology* 206:355–365.

Hynek, S. A., B. H. Passey, J. L. Prado, F. H. Brown, T. E. Cerling, and J. Quade. 2012. Small mammal carbon isotope ecology across the Miocene–Pliocene boundary, northwestern Argentina. *Earth and Planetary Science Letters* 321-322:177–188.

Jenkins, S. G., S. T. Partridge, T. R. Stephenson, S. D. Farley, and C. T. Robbins. 2001. Nitrogen and carbon isotope fractionation between mothers, neonates, and nursing offspring. *Oecologia* 129:336–341.

Johnsgard, P. A. 2002. *North American Owls: Biology and Natural History, 2nd ed.* Smithsonian Institution Press, Washington, D. C. 298 pp.

Keeling, C. D., S. C. Piper, R. B. Bacastow, M. Wahlen, T. P. Whorf, M. Heimann, and H. A. Meijer. 2005. Terrestrial biosphere and oceans from 1978 to 2000 : observations and carbon cycle implications; pp. 83–113 in J. R. Ehleringer, T. E. Cerling, and M. D. Dearing (eds.), *A History of Atmospheric CO2 and its Effects on Plants, Animals, and Ecosystems*. Springer-Verlag, New York, NY.

Koch, P. L., N. Tuross, and M. L. Fogel. 1997. The effects of sample treatment and diagenesis on the isotopic integrity of carbonate in biogenic hydroxylapatite. *Journal of Archaeological Science* 24:417–429.

Koch, P. L., N. S. Diffenbaugh, and K. A. Hoppe. 2004. The effects of late Quaternary climate and pCO_2 change on C_4 plant abundance in the south-central United States. *Palaeogeography, Palaeoclimatology, Palaeoecology* 207:331–357.

Koutavas, A., P. B. DeMenocal, G. C. Olive, and J. Lynch-Stieglitz. 2006. Mid-Holocene El Niño–Southern Oscillation (ENSO) attenuation revealed by individual foraminifera in eastern tropical Pacific sediments. *Geology* 34:993–996.

Koutavas, A., and S. Joanides. 2012. El Niño-Southern Oscillation extrema in the Holocene and Last Glacial Maximum. *Paleoceanography* 27(4; PA4208):1-15.

Lanzante, J. R. 2005. A cautionary note on the use of error bars. *Journal of Climate* 18:3699–3703.

Larkin, T. J., and G. W. Bomar. 1983. *Climatic Atlas of Texas*. Texas Department of Water Resources, Austin, Texas, 151 pp.

Larter, N. C., and C. C. Gates. 1994. Home-range size of wood bison: effects of age, sex, and forage availability. *Journal of Mammalogy* 75:142–149.

Leduc, G., L. Vidal, O. Cartapanis, and E. Bard. 2009. Modes of eastern equatorial Pacific thermocline variability: Implications for ENSO dynamics over the last glacial period. *Paleoceanography* 24(3; PA3202):1-14.

Lee-Thorp, J. A., and P. B. Beaumont. 1995. Vegetation and seasonality shifts during the late Quaternary deduced from $^{13}C/^{12}C$ ratios of grazers at Equus Cave, South Africa. *Quaternary Research* 43:426–432.

MacFadden, B. J., T. E. Cerling, and J. Prado. 1996. Cenozoic terrestrial ecosystem evolution in Argentina: evidence from carbon isotopes of fossil mammal teeth. *Palaios* 11:319–327.

McLean, B. S., and S. D. Emslie. 2012. Stable isotopes reflect the ecological stability of two high-elevation mammals from the late Quaternary of Colorado. *Quaternary Research* 77:408–417.

McNab, B. K. 1963. Bioenergetics and the dermination of home range size. *The American Naturalist* 97:133–140.

Means, L. L. 1952. On thunderstorm forecasting in the central United States. *Monthly Weather Review* 80:165–189.

Medina, E., G. Montes, E. Guevas, and Z. Rokzandic. 1986. Profiles of CO_2 concentration and $\delta^{13}C$ values in tropical rain forests of the upper Rio Negro Basin, Venezuela. *Journal of Tropical Ecology* 2:207–217.

Mitchell, M. J., R. W. Arritt, and K. Labas. 1995. A climatology of the warm season Great Plains low-level jet using wind profiler observations. *Weather and Forecasting* 10:576–591.

Morgan, R. G. 1980. Bison movement patterns on the Canadian plains: an ecological analysis. *Plains Anthropologist* 25:143–160.

Ode, D. J., L. L. Tieszen, and J. C. Lerman. 1980. The seasonal contribution of C_3 and C_4 plant species to primary production in a mixed prairie. *Ecology* 61:1304–1311.

Overpeck, J. T., R. S. Webb, and T. Webb III. 1992. Mapping eastern North American vegetation change of the past 18 ka : No-analogs and the future. *Geology* 20:1071–1074.

Paruelo, J. M., W. K. Lauenroth, S. E. Applications, and N. Nov. 1996. Relative abundance of plant functional types in grasslands and shrublands of North America. *Ecological Applications* 6:1212–1224.

Passey, B. H., T. F. Robinson, L. K. Ayliffe, T. E. Cerling, M. Sponheimer, M. D. Dearing, B. L. Roeder, and J. R. Ehleringer. 2005. Carbon isotope fractionation between diet, breath CO_2, and bioapatite in different mammals. *Journal of Archaeological Science* 32:1459–1470.

Petit, J. R., J. Jouzel, D. Raynaud, N. I. Barkov, J. M. Barnola, I. Basile, M. Bender, J. Chappellaz, M. Davis, G. Delaygue, C. Ritz, M. Delmotte, V. M. Kotlyakov, M. Legrand, V. Y. Lipenkov, C. Lorius, L. Pepin, E. Saltzman, and M. Stievenard. 1999. Climate and atmospheric history of the past 420,000 years from the Vostok ice core, Antarctica. *Nature* 399:429–436.

Podlesak, D. W., A.-M. Torregrossa, J. R. Ehleringer, M. D. Dearing, B. H. Passey, and T. E. Cerling. 2008. Turnover of oxygen and hydrogen isotopes in the body water, CO_2, hair, and enamel of a small mammal. *Geochimica et Cosmochimica Acta* 72:19–35.

Probert, R. J. 2000. The role of temperature in the regulation of seed dormancy and germination; pp. 261–292 in M. Fenner (ed.), *Seeds: The Ecology of Regeneration in Plant Communities, 2nd ed*. CABI Publishing, Oxford, UK.

Rathcke, B., and E. P. Lacey. 1985. Phenological patterns of terrestrial plants. *Annual Review of Ecology and Systematics* 16:179–214.

Raynal, D. J., and F. A. Bazzaz. 1975. Interference of winter annuals with *Ambrosia artemisiifolia* in early successional fields. *Ecology* 56:35–49.

Reimer, P. J., M. G. L. Baillie, E. Bard, A. Bayliss, J. W. Beck, P. G. Blackwell, C. Bronk Ramsey, C. E. Buck, G. S. Burr, R. L. Edwards, M. Friedrich, P. M. Grootes, T. P. Guilderson, I. Hajdas, T. J. Heaton, A. G. Hogg, K. A. Hughen, K. F. Kaiser,

B. Kromer, F. G. McCormac, S. W. Manning, R. W. Reimer, D. A. Richards, J. R. Southon, S. Talamo, C. S. M. Turney, J. van der Plicht, and C. E. Weyhenmeyer. 2009. IntCal09 and Marine09 radiocarbon age calibration curves, 0-50,000 years cal. BP. *Radiocarbon* 51:1111–1150.

Rogers, K. L., and Y. Wang. 2002. Stable isotopes in pocket gopher teeth as evidence of a late Matuyama climate shift in the southern Rocky Mountains. *Quaternary Research* 57:200–207.

Rohde, A., and R. P. Bhalerao. 2007. Plant dormancy in the perennial context. *Trends in Plant Science* 12:217–223.

Royer, A., C. Lécuyer, S. Montuire, R. Amiot, S. Legendre, G. Cuenca-Bescós, M. Jeannet, and F. Martineau. 2013. What does the oxygen isotope composition of rodent teeth record? *Earth and Planetary Science Letters* 361:258–271.

Sage, R. F., P.-A. Christin, and E. J. Edwards. 2011. The C_4 plant lineages of planet Earth. *Journal of Experimental Botany* 62:3155–3169.

Sankaran, M., N. P. Hanan, R. J. Scholes, J. Ratnam, D. J. Augustine, B. S. Cade, J. Gignoux, S. I. Higgins, X. Le Roux, F. Ludwig, J. Ardo, F. Banyikwa, A. Bronn, G. Bucini, K. K. Caylor, M. B. Coughenour, A. Diouf, W. Ekaya, C. J. Feral, E. C. February, P. G. H. Frost, P. Hiernaux, H. Hrabar, K. L. Metzger, H. H. T. Prins, S. Ringrose, W. Sea, J. Tews, J. Worden, and N. Zambatis. 2005. Determinants of woody cover in African savannas. *Nature* 438:846–849.

Schiller, A., U. Mikolajewicz, and R. Voss. 1997. The stability of the North Atlantic thermohaline circulation in a coupled ocean-atmosphere general circulation model. *Climate Dynamics* 13:325–347.

Schmidly, D. J. 1994. *The Mammals of Texas, Revised Edition*. University of Texas Press. Austin, TX. 501 pp.

Sherry, R. A., E. Weng, J. A. Arnone III, D. W. Johnson, D. S. Schimel, P. S. Verburg, L. L. Wallace, and Y. Luo. 2008. Lagged effects of experimental warming and doubled precipitation on annual and seasonal aboveground biomass production in a tallgrass prairie. *Global Change Biology* 14:2923–2936.

Shuman, B., T. Webb, P. Bartlein, and J. W. Williams. 2002. The anatomy of a climatic oscillation : vegetation change in eastern North America during the Younger Dryas chronozone. *Quaternary Science Reviews* 21:1777–1791.

Smeins, F. E., T. W. Taylor, and L. B. Merrill. 1976. Vegetation of a 25-year exclosure on the Edwards Plateau, Texas. *Journal of Range Management* 29:24–29.

Smith, C. S. 2011. *Stable carbon isotope analysis of modern leporids to assess their usefulness as fine-grained ecological proxies to reconstruct local paleoecology*. University of Texas at San Antonio. Unpublished Master's Thesis. 101 pp.

Steinbeiss, S., V. M. Temperton, and G. Gleixner. 2008. Mechanisms of short-term soil carbon storage in experimental grasslands. *Soil Biology and Biochemistry* 40:2634–2642.

Teeri, J. A., and L. G. Stowe. 1976. Climatic patterns and the distribution of C_4 grasses in North America. *Oecologia* 23:1–12.

Tieszen, L. L., D. J. Ode, P. W. Barnes, and P. M. Bultsma. 1980. Seasonal variation in C_3 and C_4 biomass at the Ordway Prairie and selectivity by bison and cattle; pp. 165–174 in C. L. Kucera (ed.), *Proceedings of the 7th North American Prairie Conference*. Southwest Missouri State University. Springfield, Missouri.

Toomey, R. S. I. 1993. *Late Pleistocene and Holocene faunal and environmental changes at Hall's Cave, Kerr County, Texas*. The University of Texas at Austin. Unpublished doctoral dissertation. 560 pp.

Turkowski, F. J. 1975. Dietary Adaptability of the Desert Cottontail. *The Journal of Wildlife Management* 39:748–756.

Ugan, A., and J. Coltrain. 2011. Variation in collagen stable nitrogen values in black-tailed jackrabbits (*Lepus californicus*) in relation to small-scale differences in climate, soil, and topography. *Journal of Archaeological Science* 38:1417–1429.

Ungar, P. S. 2010. *Mammal Teeth*. The Johns Hopkins University Press. Baltimore, MD. 304 pp.

Van Auken, O. W. 1997. Germination requirements of aerial chasmogamous florets and seeds of *Nassella leucotricha* (Poaceae). *The Southwestern Naturalist* 42:194–200.

Vander Wall, S. B. 1990. *Food Hoarding in Animals*. The University of Chicago Press. Chicago, IL. 445 pp.

Volaire, F., and M. Norton. 2006. Summer dormancy in perennial temperate grasses. *Annals of Botany* 98:927–933.

Whitlock, M. C. and D. Schluter. 2009. *The Analysis of Biological Data*. Roberts and Company Publishers. Greenwood Village, CO. 700 pp.

Yu, Z., and H. E. W. Jr. 2001. Response of interior North America to abrupt climate oscillations in the North Atlantic region during the last deglaciation. *Earth-Science Reviews* 52:333–369.

Zimmerman, J. K., and J. R. Ehleringer. 1990. Carbon isotope ratios are correlated with irradiance levels in the Panamanian orchid *Catasetum viridiflavum*. *Oecologia* 83:247–249.